İSTANBUL TECHNICAL UNIVERSITY ★ INSTITUTE OF SCIENCE AND TECHNOLOGY

BRAGG FIBERS

M.Sc. Thesis by
Aslı ÜNLÜGEDİK, B.Sc.

(504041302)

Date of submission : 7 May 2007

Date of defence examination: 13 June 2007

Supervisor (Chairman): Prof. Dr. Ercan TOPUZ (İ.T.U.)

Members of the Examining Committee Prof.Dr. İbrahim AKDUMAN (İ.T.U.)

Assoc. Prof.Dr. Özlem ÜNVERDİ (Y.T.U.)

JUNE 2007

İSTANBUL TEKNİK ÜNİVERSİTESİ ★ FEN BİLİMLERİ ENSTİTÜSÜ

BRAGG FİBERLER

YÜKSEK LİSANS TEZİ
Müh. Aslı ÜNLÜGEDİK
(504041302)

Tezin Enstitüye Verildiği Tarih : 7 Mayıs 2007
Tezin Savunulduğu Tarih : 13 Haziran 2007

Tez Danışmanı :	**Prof.Dr. Ercan TOPUZ (İ.T.Ü.)**
Diğer Jüri Üyeleri	**Prof.Dr. İbrahim AKDUMAN (İ.T.Ü.)**
	Y.Doç.Dr. Özlem ÜNVERDİ (Y.T.Ü.)

HAZİRAN 2007

ACKNOWLEDGEMENTS

I would like to thanks Professor Ercan Topuz for being my advisor and mentor. I feel privileged and honored to be his student. Next, I would like to express my deep appreciation to Serkan Şimşek and Mehmet Çayören who have kindly shared their knowledge and wisdom with me. Also, I would like to thank Turkish Scientific and Research Council (TUBITAK) for their support.

Finally, I would like to bestow my special thanks upon my mother Zekiye, my father Hüseyin, my elder sister Elif and my younger sister Özlem, for their love. It is hard to think of life without them.

I would like to thank to Ender Yılmaz, expressing my deep appreciation for his suggestion and encouragement. He always kept me on track with his love and care.

JUNE, 2007 **ASLI ÜNLÜGEDİK**

CONTENTS

ABBREVIATIONS

TIR	: Total Internal Reflection
PBG	: Photonic Band Gap effect
HIC	: High-Index Core fibers
IG	: Index Guiding fibers
HF	: Holey Fibers
BG	: Bandgap-Guiding
PCF	: Photonic Crystal Fiber
MSF	: Microstructured Fiber
MOP	: Microstructured Optical Fiber
HNA	: High Numerical Aperture
HNL	: Highly Non- Linear
LMA	: Large Mode Area
LIC	: Low-index Core
BF	: Bragg Fiber
AG	: Air-Guiding
HC	: Hollow-Core
TE	: Transverse Electric
TM	: Transverse Magnetic
LP	: Linearly Polarized
FDTD	: Finite Difference Time Domain

LIST OF FIGURES

Page No

LIST OF SYMBOLS

Λ	: A constant shows the period
l_1	: Thickness of first cladding region
l_2	: Thickness of second cladding region
k	: Wave number
β	: Propagation constant
Ψ_Z	: z component of electric or magnetic field
ω	: Angular frequency
l	: Azimuthal dependence
n_c	: Refractive index of the core
n_1, n_2	: Refractive index of the first and second cladding layer respectively
ψ	: Phase of the field
A_i, B_i, C_i, D_i	: Constants within the ith layer
f_{TE}, f_{TM}	: Amplitudes of TM and TE component within the Bragg cladding region
K_{TM}, K_{TE}	: Bloch (Floquet) constant
λ	: Wavelength

BRAGG FİBERLER

ÖZET

Bu tezde Bragg fiberler çalışılmıştır. Bragg fiber düşük kırılım indisli çekirdek (hava gibi) ve bu çekirdeği çevreleyen periyodik katmanlardan oluşur. Bu periyodik katmanlar yüksek ve düşük kırılım indisine sahip malzemelerden oluşur. Periyodik katmanların kırılım indisleri (kılıf bölgesi) çekirdek bölgesinin kırılım indisinden daha büyüktür.

Silindirik yapıdaki Bragg fiberin tam çözümü düzlemsel Bragg dalga kılavuzunun analizinden zordur. Bragg fiberlerde kılavuzlanan modlari asimtotik limitte analiz etmek tam çözümde karşılaşılan sorunu çözmeye ve tam çözümde elde edilen sonuçlara çok iyi yaklaşan sonuçlar bulmaya sebep olur.

Bu çalışmanın ilk kısmında Bragg fiber yapısı ve kılavuzlanan modlari bulmak için kullanılan metodlar açıklanmıştır. Asimtotik analiz metodu ve yeni bir yaklaşım olan asimtotik matris formalizasyonu anlatılmıştır. Asimtotik matris formalizasyonunda ilk bir kaç dielektrik katman tam çözümle daha sonraki katmanlar ise asimtotik limitte analiz edilerek Bragg fiberin dağılım bagintisi bulunur.

BRAGG FIBERS

SUMMARY

Bragg Fiber is studied in this thesis. Bragg fibers consist of a low index core, including air, which is surrounded by periodic layers. These periodic layers have a property such that they can be formed from high and low refractive index materials. The refractive indexes of periodic layers, which are called, cladding region, have higher refractive index than that of core region.

The exact theoretical analysis of cylindrical Bragg fibers is considerably more complicated than the analysis of the planar Bragg waveguides. Using asymptotic limit to analyze the guided mode in Bragg fiber simplifies the problem and provides an excellent solution which is found from exact analysis.

In the first part of this investigation, Bragg fiber structure and the methods which are used to determine guided modes, are explained. The asymptotic analysis is explained and then a new approach called asymptotic matrix formalism is used. Asymptotic matrix formalism is an approach in which the first several dielectric layers are solved exactly and the rest of the dielectric cladding structures are approximated in the asymptotic limit to find the dispersion relation of Bragg fibers.

1. INTRODUCTION

For the last decade, scientists are interested in the optical properties of materials after the mechanical and electrical properties of materials were extensively studied. From the studies of optical properties the aim is: to prohibit the propagation of light, or to allow it only in certain directions at certain frequencies or to confine light in specified areas [1]. Following studies a new and an important concept has been envolved which is called Photonic Crystals.

Crystal is defined as a periodic structure with an arrangement of atoms and molecules which causes a periodic potential. Investigation of the energy band diagram of crystals shows that there are gaps where electrons are forbidden to propagate in certain directions at certain frequencies. If the lattice potential is strong enough, a complete band gap can be observed where forbidden extends to all directions.

In optics, periodic potential is due to a lattice of macroscopic dielectric media instead of atoms and these structures are called “photonic crystals”, or equally called “photonic band gap materials”. In photonic crystals, different dielectric constants of the materials causes frequency ranges where no electromagnetic eigenmodes exist which are called photonic band gaps.

The photonic band gap effect was first described in 1987 by Yablonovitch and John. In this work novel periodic materials were studied in terms of the control of spontaneous emission and the localization of light [2-4].

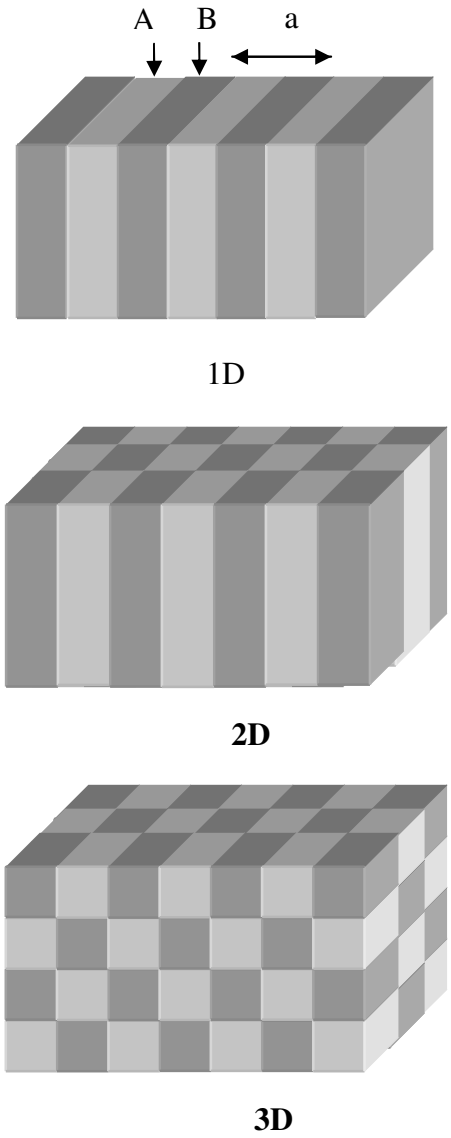

Figure 1.1 : Schematic illustration of one dimensional, two dimensional and three dimensional photonic crystals. a is the lattice constant.

Photonic crystals are composed of arrays of materials which have different refractive indices. A and B in figure (1.1) show the different layers and the symbol 'a' shows the period of the layer called lattice constant. In a typical crystal the lattice constant is on the order of angstroms, for photonic crystals it is on the order of the wavelength of the relevant electromagnetic waves.

Photonic or microstructured fiber or microstuctured optical fiber can be classified into two groups according to guiding behaviour of light in the fiber. These groups are

classified according to their confinement method. Confinement methods are total internal reflection (TIR) and photonic band gap effect (PBG). In the physical mechanism of total internal reflection a higher refractive index of the core is used compared to the surrounding layer material. In the first group, fibers are referred as High-Index Core (HIC) fibers, Index Guiding (IG) fibers or Holey Fibers (HF). In the second group, fibers are called as Photonic Band Gap (PBG) fibers or Bandgap-Guiding (BG) fibers. These two groups can be also divided into subgroups, and these subgroups are determined according to the dimensions of the fiber structures and their specific properties [4]. These classes are shown in the figure (1.2):

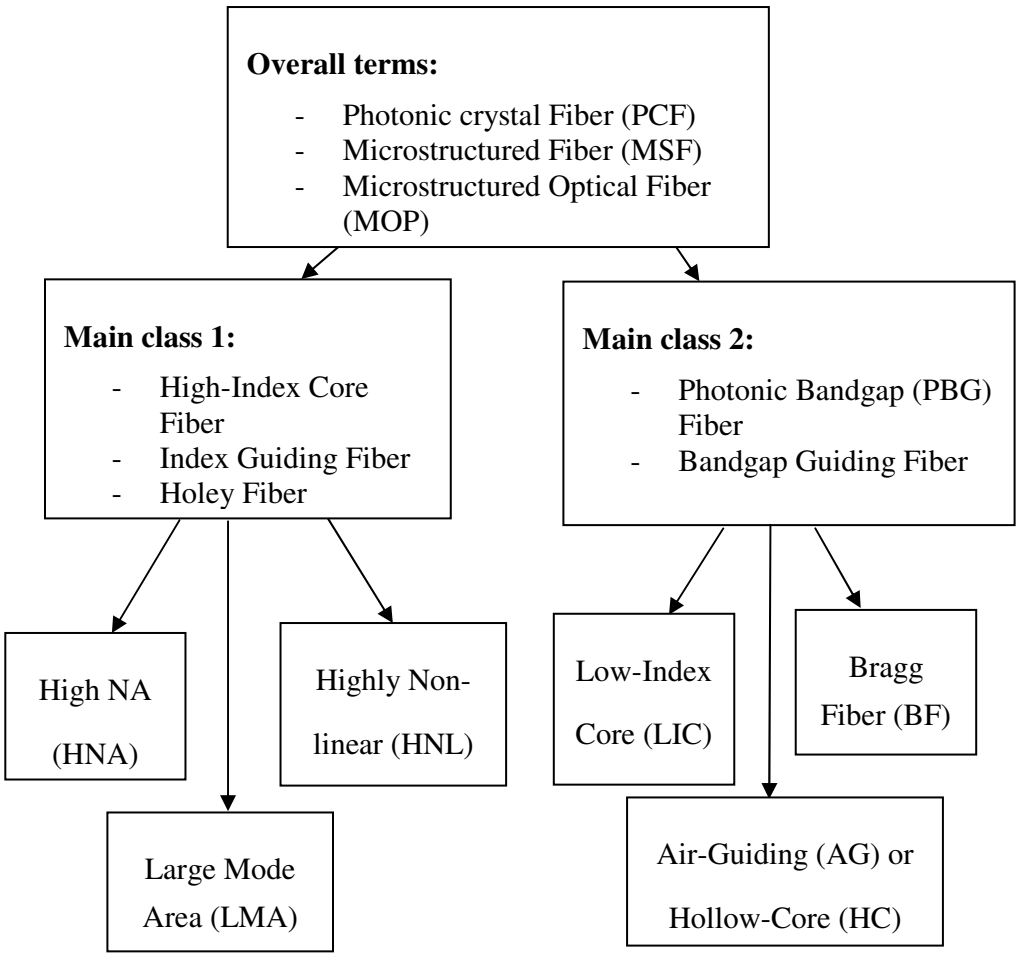

Figure 1.2 : Diagram showing the most commonly used terms and typical structures for the major classes and sub-classes of photonic crystal fibers.[4]

1.1 Bragg Fibers

Bragg fibers are the subclasses of PBG fibers. They have rotational symmetry. Bragg fibers are different from the other subclasses of PBG fibers due to their ring structures. Other subclasses of PBG fibers have individual holes which are distributed in the cladding. Bragg fibers were first explained by Yeh et al in a theoretical paper [5] in 1978.

In the cladding region of Bragg fibers light is guided by cylindrical Bragg reflection method instead of total internal reflection method. Total internal reflection method requires a core with a higher refractive index than refractive index of the cladding layers. However, Bragg reflection dielectric waveguide causes lossy (leaky) modes, and these modes are required for the inner media, called core, that has a lower refractive index than the surrounding outer media, called cladding. There are some situations where guiding power in a lower index of the core, compared to the surrounding media is required. An example for this situation is the waveguide laser in which the core layer is air. The advantages of this kind of fibers are lower absorption loss and higher threshold power for nonlinear effects

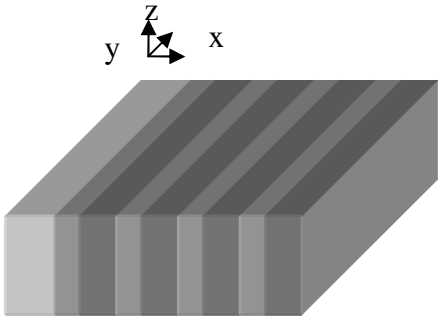

(a)

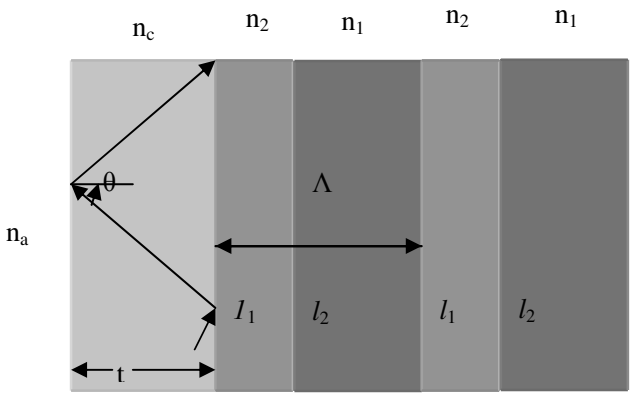

(b)

Figure 1.3 : A Bragg reflection (slab) dielectric waveguide (a), top view of a Bragg reflection (slab) dielectric waveguide (b).

In figure (1.3) the refractive index have properties as $n_a<n_c<n_1$, n_2.

The principle of Bragg fiber is similar to a multilayer planar stack. Bragg fibers consist of a low index core and this core is bounded by media that have higher refractive indices n_1 and n_2 with thickness of l_1, l_2. The symbol Λ is the sum of l_1 and l_2.

The exact solution of Bragg fibers is more complicated than the analysis of planar Bragg waveguides. Finding an equation that determines the confined modes is difficult because Bloch theorem which is applied to planar Bragg fiber structures, cannot be used for the cylindrically symmetric structures. For the exact analysis of this kind of fiber the idea depends on minimizing the outward flowing power flux by choosing the thickness of the cladding layers[5]. In order to accomplish this requirement the thickness should be chosen such that the optimum confinement is achieved. Moreover, optimum confinement is achieved if the cladding bi-layers are of half-wave thickness; called quarter-wave thickness condition:

$$k_1 * l_1 = k_2 * l_2 = \Pi/2 \qquad \textbf{(1.1)}$$

Effective index of a guided mode in Bragg fibers can be found by equation (1.1).

Transverse electric (TE) and transverse magnetic (TM) modes of Bragg fibers are non-degenerate, unlike linearly polarized (LP) modes of conventional fibers. Bragg fibers can be designed for a single guided mode without azimuthal dependence, and with this property undesirable polarization dependent effects can be eliminated. A single mode fiber can transmit light without broadening which is caused from modal dispersion. Also it is shown that Bragg fiber can be used as a mode filter to select a particular mode from an ensemble of modes. Consequently, Bragg fibers support a single transverse electric and transverse magnetic mode which means Bragg fibers are free of polarization mode dispersion [6,7]. A Bragg fiber is not only formed with an air core, they could also be formed with silica/doped silica core and a periodic cladding in which case the core has the lowest refractive index of the structure.

2. THEORY OF BRAGG FIBER

In 1976, Yeh and Yariv studied slab in which light is guided with a lower refractive index core compared to the refractive index of cladding [8]. The information of the quarter-wave layers is required for the best Bragg confinement was arised from this study.

Within the last decade, the research of cylindrically symmetric dielectric waveguides has been recognized as an important area of optical technology. Studies of cylindrically symmetric dielectric waveguides showed that their theory is similar to planar slab waveguides. Their operation relies on light being guided by the layer, core, which has a higher refractive index than that of surroundings, namely cladding. In Bragg fibers light guided by the low-index core, and the core is bounded by an alternating cladding region which have high and low refractive indices.

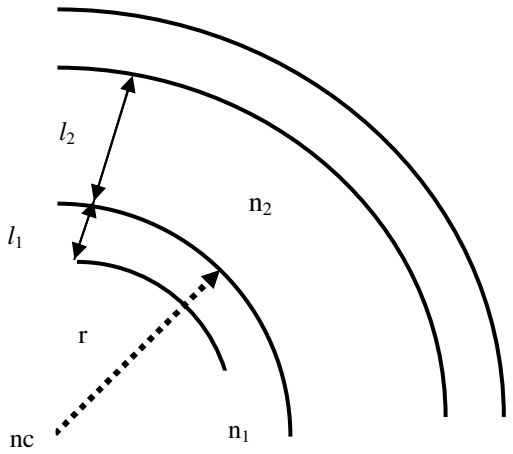

Figure 2.1 : Schematic of Bragg fiber cross section.

In figure (2.1), n_1 and n_2 are high refractive index cladding and low refractive index cladding, respectively. Also l_1 and l_2 are the thickness of high and low refractive index cladding structures, respectively. In order to solve the wave equation, boundary conditions are used at the interface between neighbor dielectric layers. After the boundary condition is applied the wave equation becomes:

$$\psi_z = \left[AJ_l(k_i r) + BY_l(k_i r)\right]\exp(-il\theta)\exp(i(\beta z - \omega t)) \quad \textbf{(2.1)}$$

where Ψ_z denotes E_z or H_z and wave vector k_i = sqrt $(n_i^2(w/c)^2-\beta^2)$. ω is defined as angular frequency and β shows the propagation constant.

In order to find the propagation constant of excited modes in Bragg fibers, several different approaches are utilized such as exact solution, asymptotic approach, matrix asymptotic approach, FDTD method and Galerkin method.

Yeh and Yariv [5] showed that there exists confined modes in Bragg fibers and the exact solution can be found by minimizing the radiation loss in radial direction. The exact theoretical analysis of Bragg fibers is complicated because the Bloch theorem can no longer be applied for cylindrical coordinates. Different analysis techniques are used to solve the problem in an uncomplicated way, and asymptotic approach is the one of these solution methods. Using asymptotic approach, the problem can be modified into a simple form and the approach provides a very close answer that is found with the exact analysis.

2.1 The Exact Theoretical Analysis

In Bragg fibers most of the light confined within the air core. The explanation of physical mechanism of Bragg fiber is more complicated than that of conventional fiber. Yeh studied the exact theoretical analysis [5] and defined matrix formalism and matrix elements coming from Maxwell equations. Four independent parameters in each layer were used for the solution of Maxwell equations and the parameters of adjacent layers were related to a 4x4 matrix. The confined modes in a Bragg fiber were treated as quasi-modes. Propagation constant and field distribution can be found by minimizing the radiation loss.

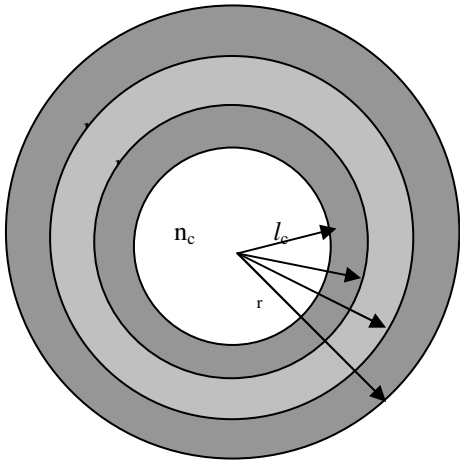

Figure 2.2 : Schematic of Bragg fiber.

The index profile is considered as given:

$$n(r) = \begin{cases} n_{C,} & 0 \le r \le r_1 \\ n_2, & r_1 \le r \le r_2 \\ n_1, & r_2 \le r \le r3 \\ n_2, & r_3 \le r \le r_4 \\ n_1, & r_4 \le r \le r_5 \\ \text{etc.} & \end{cases}$$

If the z-axis is defined as the direction of propagation, every field component is defined as:

$$\psi(r,\theta,z,t) = \psi(r,\theta)\exp(i(\beta z - \omega t)) \qquad \textbf{(2.2)}$$

Where Ψ is used for E_z, E_r, E_θ, H_z, H_r, H_θ. The symbol β is used for the propagation constant, and w is the angular frequency. In axially symmetric optical fibers, the refractive index is expressed as n(r) and does not depend on θ. The transverse electromagnetic fields are related to E_z and H_z as:

$$E_r = \frac{i\beta}{(\omega^2\mu\varepsilon - \beta^2)}\left(\frac{\partial E_z}{\partial r} + \frac{\omega\mu}{\beta}\frac{\partial}{r\partial\theta}H_z\right) \qquad \textbf{(2.3)}$$

$$E_\theta = \frac{i\beta}{\left(\omega^2\mu\varepsilon - \beta^2\right)}\left(\frac{\partial}{r\partial\theta}E_z - \frac{\omega\mu}{\beta}\frac{\partial}{\partial r}H_z\right) \quad \textbf{(2.4)}$$

$$H_r = \frac{i\beta}{\left(\omega^2\mu\varepsilon - \beta^2\right)}\left(\frac{\partial H_z}{\partial r} - \frac{\omega\varepsilon}{\beta}\frac{\partial}{r\partial\theta}E_z\right) \quad \textbf{(2.5)}$$

$$H_\theta = \frac{i\beta}{\left(\omega^2\mu\varepsilon - \beta^2\right)}\left(\frac{\partial}{r\partial\theta}H_z + \frac{\omega\varepsilon}{\beta}\frac{\partial}{\partial r}E_z\right) \quad \textbf{(2.6)}$$

In axially symmetric fiber, the azimuthal dependence of the electromagnetic field is shown as cos(nθ + ψ) or sin(nθ + ψ). The symbol n is an integer and ψ denotes the phase. E_z (r, θ) and H_z (r, θ) are satisfying the wave equation as:

$$\left[\nabla_t^2 + \left(\omega^2\mu\varepsilon - \beta^2\right)\right]\{E_z, H_z\} = 0 \quad \textbf{(2.7)}$$

∇_t is the transverse Laplacian operator and is equal to ($\nabla^2 - \frac{\partial^2}{\partial z^2}$).

The general solutions of E_z and H_z are:

$$E_z = \left[AJ_l(kr) + BY_l(kr)\right]\cos(l\theta + \phi) \quad \textbf{(2.8)}$$

$$H_z = \left[CJ_l(kr) + DY_l(kr)\right]\cos(l\theta + \psi) \quad \textbf{(2.9)}$$

Where A, B, C, D, ϕ, ψ are constants and *l* is an integer. k is the wave number which has a value:

$$k = \left(\omega^2\mu\varepsilon - \beta^2\right)^{\frac{1}{2}} \quad \textbf{(2.10)}$$

If the boundary conditions are applied at interface at r = ρ, the solutions are:

$$E_z = \left[A_1 J_l(k_1 r) + B_1 Y_l(k_1 r)\right]\cos\left(l\theta + \phi_1\right) \quad \textbf{(2.11)}$$

$$E_z = \left[A_2 J_l(k_2 r) + B_2 Y_l(k_2 r)\right]\cos(l\theta + \phi_2) \quad \textbf{(2.12)}$$

$$H_z = [C_1 J_l(k_1 r) + D_1 Y_l(k_1 r)]\cos(l\theta + \psi_1) \quad \textbf{(2.13)}$$

$$H_z = [C_2 J_l(k_2 r) + D_2 Y_l(k_2 r)]\cos(l\theta + \psi_2) \quad \textbf{(2.14)}$$

The first equations of E_z and H_z are in the region of $r < \rho$, whereas the second equations are in the region of $r > \rho$. k used in equations is equal to:

$$k = \left((\omega / c)^2 \mu_i \varepsilon_i - \beta^2\right)^{\frac{1}{2}} \quad \text{, i = 1, 2.} \quad \textbf{(2.15)}$$

From the boundary conditions we know that E_z, E_θ, H_z, H_θ are continuous at all interfaces. The information extracted from this continuity a 4x4 matrix is found which relates the constants of adjacent layers as:

$$\begin{pmatrix} A_2 \\ B_2 \\ C_2 \\ D_2 \end{pmatrix} = M \begin{pmatrix} A_1 \\ B_1 \\ C_1 \\ D_1 \end{pmatrix} \quad \textbf{(2.16)}$$

2.1.1 Matrix M

When the boundary condition is applied at the point $r = \rho$, E_z should be continuous, we can find equations such as:

$$[A_1 J_l(k_1\rho) + B_1 Y_l(k_1\rho)]\cos(l\theta + \phi_1) = [A_2 J_l(k_2\rho) + B_2 Y_l(k_2\rho)]\cos(l\theta + \phi_2) \quad \textbf{(2.17)}$$

The equation given above should be satisfied for all θ. Subsequently, we reach a condition as: $Ø_1 = Ø_2$. When the boundary condition is applied for H_z, it can be found that $\psi_1 = \psi_2$. After these adjustments E_z and H_z is found as given below:

$$[A_1 J_l(k_1\rho) + B_1 Y_l(k_1\rho)] = [A_2 J_l(k_2\rho) + B_2 Y_l(k_2\rho)] \quad \textbf{(2.18)}$$

$$[C_1 J_l(k_1\rho) + D_1 Y_l(k_1\rho)] = [C_2 J_l(k_2\rho) + D_2 Y_l(k_2\rho)] \quad \textbf{(2.19)}$$

From the continuity condition of E_θ we can find the following equation

$$\sin(l\theta+\phi)=\pm\cos(l\theta+\psi) \tag{2.20}$$

Equation (2.20) is required a condition as:

$$\phi=\psi\pm\frac{\pi}{2} \tag{2.21}$$

Wave equations can be divided into two categories, first one can be written as:

$$E_z=\left[AJ_l(kr)+BY_l(kr)\right]\cos(l\theta) \tag{2.22}$$

$$H_z=\left[CJ_l(kr)+DY_l(kr)\right]\sin(l\theta) \tag{2.23}$$

And the second categories of equations are:

$$E_z=\left[AJ_l(kr)+BY_l(kr)\right]\sin(l\theta) \tag{2.24}$$

$$H_z=\left[CJ_l(kr)+DY_l(kr)\right]\cos(l\theta) \tag{2.25}$$

If boundary condition is applied to equation (2.22) and (2.23) the following equations are found:

$$A_1J_l(k_1\rho)+B_1Y_l(k_1\rho)+0+0=0 \tag{2.26}$$

$$\frac{\omega\varepsilon_1}{k_1\beta}A_1J_l'(k_1\rho)+\frac{\omega\varepsilon_1}{k_1\beta}B_1Y_l'(k_1\rho)+\frac{l}{k_1^2\rho}C_1J_l(k_1\rho)+\frac{l}{k_1^2\rho}D_1Y_l(k_1\rho)=0 \tag{2.27}$$

$$0+0+C_1J_l(k_1\rho)+D_1Y_l(k_1\rho)=0 \tag{2.28}$$

$$\frac{l}{k_1^2\rho}A_1J_l(k_1\rho)+\frac{l}{k_1^2\rho}B_1Y_l(k_1\rho)+\frac{\omega\mu_1}{k_1\beta}C_1J_l'(k_1\rho)+\frac{\omega\mu_1}{k_1\beta}D_1Y_l'(k_1\rho)=0 \tag{2.29}$$

These equations can be written in matrix form:

$$M(i,\rho)=\begin{bmatrix} J_l(k_i\rho) & Y_l(k_i\rho) & 0 & 0 \\ \frac{\omega\varepsilon_i}{\beta k_i}J_l'(k_i\rho) & \frac{\omega\varepsilon_i}{\beta k_i}Y_l'(k_i\rho) & \frac{l}{k_i^2\rho}J_l(k_i\rho) & \frac{l}{k_i^2\rho}Y_l(k_i\rho) \\ 0 & 0 & J_l(k_i\rho) & Y_l(k_i\rho) \\ \frac{l}{k_i^2\rho}J_l(k_i\rho) & \frac{l}{k_i^2\rho}Y_l(k_i\rho) & \frac{\omega\mu_i}{\beta k_i}J_l'(k_i\rho) & \frac{\omega\mu_i}{\beta k_i}Y_l'(k_i\rho) \end{bmatrix} \quad \textbf{(2.30)}$$

$$\begin{bmatrix} E_Z \\ \frac{1}{i\beta}H_\theta \\ H_Z \\ -\frac{1}{i\beta}E_\theta \end{bmatrix} = M(i,\rho)\begin{bmatrix} A_i \\ B_i \\ C_i \\ D_i \end{bmatrix} \quad \textbf{(2.31)}$$

Where *i* is equal to 1, 2. If the value of *l* is equal to zero, the matrix is reducible, so pure transverse electric or transverse magnetic waves exist.

2.2 Asymptotic Analysis

The minimization procedure, used in the exact theoretical analysis, is easy to apply to transverse electric and transverse magnetic modes, because there is only one variable which is the propagation constant, β, that affects the radiation loss. For other types of guided modes, matrix approach is complicated, since it is a complicated process to find the eigenmodes in fiber cladding layers. Eigenmodes are easy to find when the structure is planar air core Bragg waveguide since Bloch theorem is applicable. For cylindrically symmetric Bragg fibers, Bloch theorem can no longer be applied, since the structure is not strictly periodic. Because of this problem, it is not useful to use exact theoretical approach to find mode dispersion which is found by matching the cladding and core solution at the core-cladding interface. Asymptotic approach can be used in order to overcome this problem.

In the asymptotic limit of the exact solutions of Maxwell function, Bessel function can be approximated as exp(ikr)/sqrt(r) and exp(-ikr)/sqrt(r) [9]. After this approximation eigensolutions in the cladding layer are easy to find,and the solutions are similar to the solutions of planar Bragg fibers.

For guided modes the z-dependence is shown as exp(i(βz-wt)) and the azimuthal dependence is shown as cos($l\theta$) or sin($l\theta$). After describing the cladding fields with the estimation of asymptotic limit for the Bessel functions at kr → ∞, E_z and H_z are equals to [9]:

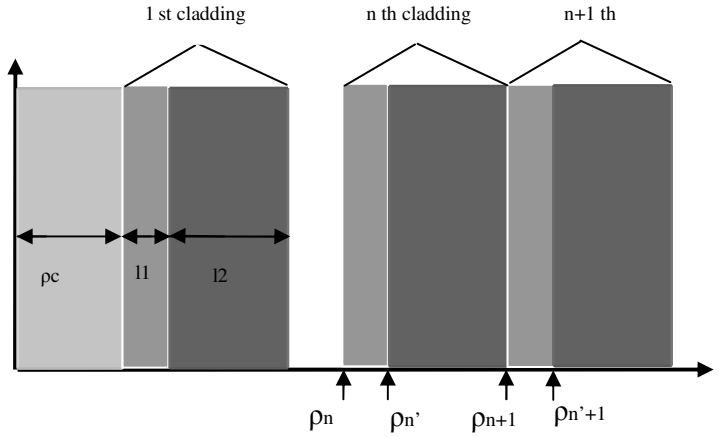

Figure 2.3 : Schematic of the r-z cross section of a Bragg fiber.

$$E_z = a_c J_l(k_c r) \qquad 0 < r < \rho_c \qquad \textbf{(2.32)}$$

$$E_z = \frac{a_n \exp[ik_1(r-\rho_n)] + b_n \exp[-ik_1(r-\rho_n)]}{\sqrt{k_1 r}} \qquad \rho_n < r < \rho_n + l_1 \qquad \textbf{(2.33)}$$

$$E_z = \frac{a'_n \exp[ik_2(r-\rho'_n)] + b'_n \exp[-ik_2(r-\rho'_n)]}{\sqrt{k_2 r}} \qquad \rho_n' < r < \rho_n' + l_2 \qquad \textbf{(2.34)}$$

$$H_z = c_c J_l(k_c r) \qquad 0 < r < \rho_1 \qquad \textbf{(2.35)}$$

$$H_z = \frac{c_n \exp[ik_1(r-\rho_n)] + d_n \exp[-ik_1(r-\rho_n)]}{\sqrt{k_1 r}} \qquad \rho_n < r < \rho_n + l_1 \qquad \textbf{(2.36)}$$

$$H_z = \frac{c'_n \exp[ik_2(r-\rho'_n)] + d'_n \exp[-ik_2(r-\rho'_n)]}{\sqrt{k_2 r}} \qquad \rho_n' < r < \rho_n' + l_2 \qquad \textbf{(2.37)}$$

Where $k_i = \sqrt{n_i^2(\omega/c)^2 - \beta^2}$. This k equation is used for both core and cladding regions. Once E_z and H_z are calculated, transverse field components can be found from the derivatives of E_z and H_z equations. After finding the equations for both E_z, E_θ, H_z, H_θ the boundary conditions are used between two neighbor dielectric layers. If the continuity requirements of E_θ and H_θ between two adjacent dielectric layers are used [9]:

If the information that E_z and H_θ are continuous is used

$$\begin{pmatrix} a_{n+1} \\ b_{n+1} \end{pmatrix} = \begin{bmatrix} A_{TM} & B_{TM} \\ B_{TM}^* & A_{TM}^* \end{bmatrix} \begin{pmatrix} a_n \\ b_n \end{pmatrix} \tag{2.38}$$

If the information that H_z and E_θ are continuous is used

$$\begin{pmatrix} c_{n+1} \\ d_{n+1} \end{pmatrix} = \begin{bmatrix} A_{TE} & B_{TE} \\ B_{TE}^* & A_{TE}^* \end{bmatrix} \begin{pmatrix} c_n \\ d_n \end{pmatrix} \tag{2.39}$$

The values of A_{TM}, A_{TE}, B_{TM}, B_{TE} are found from:

$$A_{TE} = \exp(ik_1 l_1)\left[i\frac{k_1^2 + k_2^2}{2k_1 k_2}\sin(k_2 l_2) + \cos(k_2 l_2) \right] \tag{2.40}$$

$$B_{TE} = i\exp(-ik_1 l_1)\frac{k_1^2 - k_2^2}{2k_1 k_2}\sin(k_2 l_2) \tag{2.41}$$

$$A_{TM} = \exp(ik_1 l_1)\left[i\frac{n_2^4 k_1^2 + n_1^4 k_2^2}{2n_1^2 n_2^2 k_1 k_2}\sin(k_2 l_2) + \cos(k_2 l_2) \right] \tag{2.42}$$

$$B_{TM} = i\exp(-ik_1 l_1)\frac{n_2^4 k_1^2 - n_1^4 k_2^2}{2n_1^2 n_2^2 k_1 k_2}\sin(k_2 l_2) \tag{2.43}$$

Next, the Bloch theorem is used due to the fact that A_{TM}, A_{TE}, B_{TM}, B_{TE} are the same for entire cladding region. It can be found that:

$$\begin{bmatrix} a_{n+1} \\ b_{n+1} \end{bmatrix} = (K_{TM}) \begin{bmatrix} a_n \\ b_n \end{bmatrix} \tag{2.44}$$

$$\begin{bmatrix} c_{n+1} \\ d_{n+1} \end{bmatrix} = (K_{TE}) \begin{bmatrix} c_n \\ d_n \end{bmatrix} \tag{2.45}$$

These equations mean that the fields of adjacent dielectric layers are the same except their amplitude is changed by λ_{TM} and λ_{TE} which is a result of Bloch theorem.

$$K_{TM} = \mathrm{Re}(A_{TM}) \pm \left\{ [\mathrm{Re}(A_{TM})]^2 - 1 \right\}^{1/2} \tag{2.46}$$

$$K_{TE} = \mathrm{Re}(A_{TE}) \pm \left\{ [\mathrm{Re}(A_{TE})]^2 - 1 \right\}^{1/2} \tag{2.47}$$

In the Bragg bandgap K_{TM} and K_{TE} have two real solutions, one of them has an absolute value less than one and the other has an absolute value greater than one. In order to choose the one which corresponds to decaying modes in the Bragg cladding, it is necessary to take the one that has an absolute value of less than 1. From these results it is clear that in the asymptotic limit the properties of cylindrical Bragg fiber are similar to that of planar Bragg waveguides. Results found from the asymptotic approach and results found from minimizing radiation loss have a difference less than 2% for a Bragg fiber with a small air core radius comparable to the wavelength [9]. If the core of Bragg fiber structure is too small then it is difficult to say that asymptotic approximation method is good enough to find close solutions that are subtracted from the exact analysis.

2.3 Asymptotic Matrix Formalism

As mentioned before the cladding region of Bragg fibers consists of two types of dielectric material, one cladding layer with a refractive index of n_1 and thickness l_1 and the other cladding layer that has a refractive index n_2 and thickness l_2. The asymptotic expression for field distribution of type one can be shown as [6]:

$$E_z = \frac{f_{TM}}{\sqrt{k_1 r}} \left[a_n \exp(ik_1(r - \rho_n)) + b_n \exp(-ik_1(r - \rho_n)) \right] \tag{2.48}$$

$$H_\theta = -\frac{\omega\varepsilon_0 (n_1)^2}{k_1}\frac{f_{TM}}{\sqrt{k_1 r}}\left[a_n \exp(ik_1(r-\rho_n)) - b_n \exp(-ik_1(r-\rho_n))\right] \quad \textbf{(2.49)}$$

$$H_z = \frac{f_{TE}}{\sqrt{k_1 r}}\left[c_n \exp(ik_1(r-\rho_n)) + d_n \exp(-ik_1(r-\rho_n))\right] \quad \textbf{(2.50)}$$

$$E_\theta = \frac{\omega\mu_0}{k_1}\frac{f_{TE}}{\sqrt{k_1 r}}\left[c_n \exp(ik_1(r-\rho_n)) - d_n \exp(-ik_1(r-\rho_n))\right] \quad \textbf{(2.51)}$$

The above field equations belong to the caladding layer $\rho_n \leq r < \rho_{n+1}$. The field distribution of the second layer ($\rho_n' \leq r < \rho_{n+1}'$) can be shown as:

$$E_z = \frac{f_{TM}}{\sqrt{k_2 r}}\left[a_n' \exp(ik_2(r-\rho_n')) + b_n' \exp(-ik_2(r-\rho_n'))\right] \quad \textbf{(2.52)}$$

$$H_\theta = -\frac{\omega\varepsilon_0 (n_2)^2}{k_2}\frac{f_{TM}}{\sqrt{k_2 r}}\left[a_n' \exp(ik_2(r-\rho_n')) - b_n' \exp(-ik_2(r-\rho_n'))\right] \quad \textbf{(2.53)}$$

$$H_z = \frac{f_{TE}}{\sqrt{k_2 r}}\left[c_n' \exp(ik_2(r-\rho'_n)) + d_n' \exp(-ik_2(r-\rho_n'))\right] \quad \textbf{(2.54)}$$

$$E_\theta = \frac{\omega\mu_0}{k_2}\frac{f_{TE}}{\sqrt{k_2 r}}\left[c_n' \exp(ik_2(r-\rho_n')) - d_n' \exp(-ik_2(r-\rho_n'))\right] \quad \textbf{(2.55)}$$

In these equations $k_i = \sqrt{(n_i\omega/c)^2 - \beta^2}$ where i = 1, 2.

E_z and H_θ are components of transverse magnetic and H_z and E_θ corresponds to transverse electric. In the asymptotic limit transverse magnetic (TM) and transverse electric (TE) components are decoupled, with the TM component amplitude being constant f_{TM} and TE component amplitude being constant f_{TE} [6].

Asymptotic matrix formalism is a method that several dielectric layers are assumed to be treated as exactly and the other dielectric layers are assumed to be approximated in the asymptotic limit. After doing these assumptions, guided modes in a Bragg fiber are founded by matching the exact solution in the core region with solutions founded from

the asymptotic analysis in the cladding. At the interface of the Nth core region and its neighbor first cladding region r = $\rho_N = \rho_1$. If we apply boundary condition at this interface we find matrix equation as:

$$M\left(n_N, k_N, \rho_N\right)\begin{bmatrix} A_N \\ B_N \\ C_N \\ D_N \end{bmatrix} = \begin{bmatrix} \frac{f_{TM}}{\sqrt{k_1\rho_1}}\left(K_{TM} - A_{TM} + B_{TM}\right) \\ -\frac{i\omega\varepsilon_0\left(n_1\right)^2}{k_1\beta}\frac{f_{TM}}{\sqrt{k_1\rho_1}}\left(K_{TM} - A_{TM} - B_{TM}\right) \\ \frac{f_{TE}}{\sqrt{k_1\rho_1}}\left(K_{TE} - A_{TE} + B_{TE}\right) \\ -\frac{i\omega\mu_0}{k_1\beta}\frac{f_{TE}}{\sqrt{k_1\rho_1}}\left(K_{TE} - A_{TE} - B_{TE}\right) \end{bmatrix} \quad \textbf{(2.56)}$$

From the exact analysis we know that the first core layer can be directly related to the Nth core layer as:

$$\begin{bmatrix} A_N \\ B_N \\ C_N \\ D_N \end{bmatrix} = T_{N-1}\ldots T_1\begin{bmatrix} A_1 \\ B_1 \\ C_1 \\ D_1 \end{bmatrix} \quad \textbf{(2.57)}$$

From the definition of Bessel function within the first core layer, the coefficients B_1 and D_1 are equal to zero, since $Y_1(x)$ is infinite at x = 0. Also we know that A, B coefficients comes from TM component analysis and C, D are related to TE components because of these facts we show A_1 as A_{TM} and C_1 as C_{TE}. The matrix T shown in the above equation is equal to:

$$T_i = \left[M\left(n_{i+1}, k_{i+1}, \rho_{i+1}\right)\right]^{-1} M\left(n_i, k_i, \rho_i\right) \quad \textbf{(2.58)}$$

If we rewrite the relation between Nth core layer with the first core layer we have an equation which is equal to:

$$\begin{bmatrix} A_N \\ B_N \\ C_N \\ D_N \end{bmatrix} = T_{N-1} \ldots T_2 \left[M(n_2, k_2, \rho_1) \right]^{-1} \begin{bmatrix} J_l(k_1\rho_1) & 0 \\ \frac{\omega\varepsilon_0 (n_1)^2}{k_1\beta} J_l'(k_1\rho_1) & \frac{l}{(k_1)^2\rho_1} J_l(k_1\rho_1) \\ 0 & J_l(k_1\rho_1) \\ \frac{l}{(k_1)^2\rho_1} J_l(k_1\rho_1) & \frac{\omega\mu_0}{k_1\beta} J_l'(k_1\rho_1) \end{bmatrix} \quad \textbf{(2.59)}$$

If we use this relation into equation(2.56):

$$\begin{bmatrix} J_l(k_c\rho_c) & 0 \\ \frac{\omega\varepsilon_0 (n_c)^2}{k_c\beta} J_l'(k_c\rho_c) & \frac{l}{(k_c)^2\rho_c} J_l(k_c\rho_c) \\ 0 & J_l(k_c\rho_c) \\ \frac{l}{(k_c)^2\rho_c} J_l(k_c\rho_c) & \frac{\omega\mu_0}{k_c\beta} J_l'(k_c\rho_c) \end{bmatrix} \begin{bmatrix} A_{TM} \\ C_{TE} \end{bmatrix} = T \begin{bmatrix} \frac{f_{TM}}{\sqrt{k_1\rho_1}} (K_{TM} - A_{TM} + B_{TM}) \\ -\frac{i\omega\varepsilon_0 (n_1)^2}{k_1\beta} \frac{f_{TM}}{\sqrt{k_1\rho_1}} (K_{TM} - A_{TM} - B_{TM}) \\ \frac{f_{TE}}{\sqrt{k_1\rho_1}} (K_{TE} - A_{TE} + B_{TE}) \\ -\frac{i\omega\mu_0}{k_1\beta} \frac{f_{TE}}{\sqrt{k_1\rho_1}} (K_{TE} - A_{TE} - B_{TE}) \end{bmatrix} \quad \textbf{(2.60)}$$

T matrix which is shown in the equation (2.59), is an overall transfer matrix and is equal to:

$$T = \prod_{i=2}^{N} \left[M(n_i, k_i, \rho_{i-1}) M^{-1}(n_i, k_i, \rho_i) \right] \quad \textbf{(2.61)}$$

In the equation (2.59) the fields in the first core layer are linearly related to field in the first cladding layer by transfer matrix T. In this equation we have four independent unknowns and four independent equations to find are unknowns A_{TM}, C_{TE}, f_{TM}, f_{TE}. If we can find these coefficients it is easy to find the propagation constant β and field distribution of guided modes in Bragg fiber. In order to see more clearly these equations, eight new parameters are defined [6]:

$$g_{TE}^{j} = t_{j3}(K_{TE} - A_{TE} + B_{TE}) - \frac{i\omega\mu_0}{k_{cl}^1\beta} t_{j4}(K_{TE} - A_{TE} - B_{TE}) \qquad \text{j = 1,…, 4} \quad \textbf{(2.62)}$$

$$g_{TM}^{j} = t_{j1}(K_{TM} - A_{TM} + B_{TM}) - \frac{i\omega\varepsilon_0 (n_{cl}^1)^2}{k_{cl}^1\beta} t_{j2}(K_{TM} - A_{TM} - B_{TM}) \qquad \text{j = 1,…, 4} \quad \textbf{(2.63)}$$

The values, $t_{ij,}$ shown in equations are the elements of the T matrix found from equation (2.60). With these new parameters we can rewrite equation (2.59) as:

$$\begin{bmatrix} J_l(k_c\rho_c) & 0 \\ \dfrac{\omega\varepsilon_0(n_c)^2}{k_c\beta} J_l'(k_c\rho_c) & \dfrac{l}{(k_c)^2\rho_c} J_l(k_c\rho_c) \end{bmatrix} \begin{bmatrix} A_{TM} \\ C_{TE} \end{bmatrix} = \frac{1}{\sqrt{k_1\rho_1}} \begin{bmatrix} g_{TM}^1 & g_{TE}^1 \\ g_{TM}^2 & g_{TE}^2 \end{bmatrix} \begin{bmatrix} f_{TM} \\ f_{TE} \end{bmatrix} \quad \textbf{(2.64)}$$

$$\begin{bmatrix} 0 & J_l(k_c\rho_c) \\ \dfrac{l}{(k_c)^2\rho_c} J_l(k_c\rho_c) & \dfrac{\omega\mu_0}{k_c\beta} J_l'(k_c\rho_c) \end{bmatrix} \begin{bmatrix} A_{TE} \\ C_{TM} \end{bmatrix} = \frac{1}{\sqrt{k_1\rho_1}} \begin{bmatrix} g_{TM}^3 & g_{TE}^3 \\ g_{TM}^4 & g_{TE}^4 \end{bmatrix} \begin{bmatrix} f_{TM} \\ f_{TE} \end{bmatrix} \quad \textbf{(2.65)}$$

These equations are depend on the asymptotic matrix method. If *l* is equal to zero, then we have pure TE and TM modes if the value of *l* does not equal to zero there are mixed modes. The important thing is TE and TM modes are not degenerate but are truly single mode. Therefore many undesirable phenomena caused from polarization dependency can be eliminated.

For TM modes, H_z should be equal to zero and also C_{TE} and f_{TE} are equal to zero, with this knowledge from equation (2.63) we reach the equation:

$$\frac{\omega\varepsilon_0(n_c)^2}{k_c\beta} \frac{J_0'(k_c\rho_c)}{J_0(k_c\rho_c)} = \frac{g_{TM}^2}{g_{TM}^1} \quad \textbf{(2.66)}$$

If the Bragg fiber's parameters and the frequency working with are defined, the propagation constant can be found from equation (2.65). If β_{TM} value is substitute into equation (2.65) we find A_{TM}:

$$A_{TM} = \frac{g_{TM}^1}{J_0(k_c\rho_c)\sqrt{k_1\rho_1}} f_{TM} \quad \textbf{(2.67)}$$

A_{TM} which is the mode amplitude of the first core layer, is relates to f_{TM} which is determined the fields within all the cladding layers. To obtain the TM field distribution in the cladding region, we can choose the normalization factor of the guided mode as A_{TM} is equal to 1 and should use asymptotic approach explained before. The TM field

distribution of the core region can be found from exact analysis, also we should remember that in the first core layer $A_1 = A_{TM}$ and B_1, C_1, D_1 are equal to zero.

For TE modes, A_{TM} is equal to zero and again we can choose the normalization factor of the guided mode as C_{TE} is equal to 1. If we apply the same procedure as use in TM modes we find the equations which are:

$$\frac{\omega\mu_0}{k_c\beta}\frac{J_0'(k_c\rho_c)}{J_0(k_c\rho_c)} = \frac{g_{TE}^4}{g_{TE}^3} \tag{2.68}$$

$$C_{TE} = \frac{g_{TE}^3}{J_0(k_c\rho_c)\sqrt{k_1\rho_1}} f_{TE} \tag{2.69}$$

If l is not equal to 1 there are mixed modes and solutions are more complicated than that of TM and TE modes. For simplifying the problem, some definitions are added.

$$H_{TE}^1 = J_l(k_c\rho_c)g_{TE}^4 - \frac{\omega\mu_0}{k_c\beta}J_l'(k_c\rho_c)g_{TE}^3 - \frac{l}{(k_c)^2\rho_c}J_l(k_c\rho_c)g_{TE}^1 \tag{2.70}$$

$$H_{TE}^2 = J_l(k_c\rho_c)g_{TE}^2 - \frac{\omega\varepsilon_0(n_c)^2}{k_c\beta}J_l'(k_c\rho_c)g_{TE}^1 - \frac{l}{(k_c)^2\rho_c}J_l(k_c\rho_c)g_{TE}^3 \tag{2.71}$$

$$H_{TM}^1 = J_l(k_c\rho_c)g_{TM}^4 - \frac{\omega\mu_0}{k_c\beta}J_l'(k_c\rho_c)g_{TM}^3 - \frac{l}{(k_c)^2\rho_c}J_l(k_c\rho_c)g_{TM}^1 \tag{2.72}$$

$$H_{TM}^2 = -J_l(k_c\rho_c)g_{TM}^2 + \frac{\omega\varepsilon_0(n_c)^2}{k_c\beta}J_l'(k_c\rho_c)g_{TM}^1 + \frac{l}{(k_c)^2\rho_c}J_l(k_c\rho_c)g_{TM}^3 \tag{2.73}$$

We first express A_{TM} and C_{TE} in terms of f_{TM} and f_{TE} by inverting the matrix in equation (2.64) then we use the result in equation (2.63):

$$\begin{bmatrix} H_{TM}^1 & -H_{TE}^1 \\ H_{TM}^2 & -H_{TE}^2 \end{bmatrix}\begin{bmatrix} f_{TM} \\ f_{TE} \end{bmatrix} = 0 \tag{2.74}$$

This matrix equation is used to determine the propagation constant β, in order to have nonzero solution the determinant of the matrix must be zero,

$$\frac{H_{TM}^{1}}{H_{TM}^{2}} = \frac{H_{TE}^{1}}{H_{TE}^{2}} \tag{2.75}$$

Once the Bragg fiber structure is chosen and the frequency is given, the equations defined above are only depending on the propagation constant β. After finding β and using an appropriate normalization constant, f_{TM} and f_{TE} are found as:

$$\begin{bmatrix} f_{TM} \\ f_{TE} \end{bmatrix} = \frac{l}{(k_c)^2 \rho_c} \left(J_l(k_c \rho_c)\right)^2 \sqrt{k_1 \rho_1} \begin{bmatrix} H_{TE}^{1} \\ H_{TM}^{1} \end{bmatrix} \tag{2.76}$$

If equation (2.75) is substituted into equation (2.64) the fields in the fiber core region can be obtained as:

$$\begin{bmatrix} A_{TM} \\ C_{TE} \end{bmatrix} = \begin{bmatrix} -\frac{\omega\mu}{k_c \beta} J_l'(k_c \rho_c)\left(g_{TM}^{3} H_{TE}^{1} + g_{TE}^{3} H_{TM}^{1}\right) + J_l(k_c \rho_c)\left(g_{TM}^{4} H_{TE}^{1} + g_{TE}^{4} H_{TM}^{1}\right) \\ \frac{l}{(k_c)^2 \rho_c} J_l(k_c \rho_c)\left(g_{TM}^{3} H_{TE}^{1} + g_{TE}^{3} H_{TM}^{1}\right) \end{bmatrix} \tag{2.77}$$

This matrix formalism has many advantages when compared with the asymptotic analysis. In asymptotic analysis the fiber core region exists for only one dielectric layer this causes difficulties when analysis is done for complicated Bragg fiber geometries. But, when one uses this approach there has been a chance to choose core region which contains arbitrary number of dielectric layers. Using exact solutions in the core region and choosing the number of dielectric layers that contains the core region causes more accuracy than the asymptotic analysis.

3. PLANAR STRUCTURES

As early as 1976 Yariv and co-workers have shown that a planar structure with low index 'core' region with periodic high index 'cladding' layers can support guided modes [8]. This kind of structure is called 'Bragg Fibers'. The calculation of the Bragg modes using the exact formulation [5] is rather difficult. Recently asymptotic representations have been developed which overcome this difficulty [9].

Since the asymptotic representations for the Bragg fiber heavily relies on the formulation of Bragg modes in the planar structure, it would be appropriate to treat this simpler problem first.

We consider the symmetric slab configuration shown in figure (3.1):

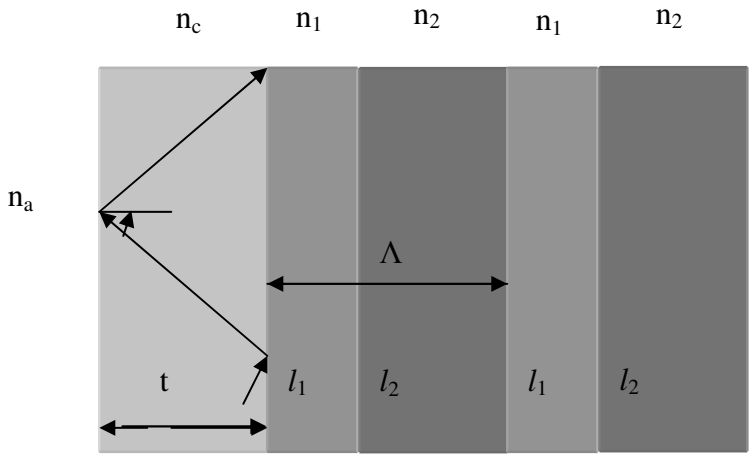

Figure 3.1 : A Bragg reflection (slab) dielectric waveguide.

Planar Bragg waveguide consists of a guiding region of thickness 2t and refractive index n_c, imbedded on both sides in symmetrical cladding regions with period $\Lambda = l_1+l_2$.

3.1 TE – TM Modes In Two Layer Structures

The investigation of propagation characteristics of TE and TM type modes in 2-layered planar Bragg structures follows similar steps, therefore in what follows the derivation of only odd-symmetric TE_Z modes will be given in detail. In this case E_X, H_Y, Ez ≡ 0 and odd-symmetry will be define via $E_Y(x) = -E_Y(-x)$, $E_Y(0) = 0$. The calculation of the eigenvalues of the Floquet modes in the periodic structure using the transfer matrix of the unit-cell depicted below.

$$E_Y = a_1 e^{-jk_1(x-t)} + b_1 e^{jk_1(x-t)} \qquad , t \le x \le t+l_1 \qquad \textbf{(3.1)}$$

$$H_Z = \frac{1}{\omega\mu}\left[k_1 a_1 e^{-jk_1(x-t)} - k_1 b_1 e^{jk_1(x-t)}\right] \qquad , t \le x \le t+l_1 \qquad \textbf{(3.2)}$$

$$E_Y = \bar{a}\, e^{-jk_2(x-(t+l_1))} + \bar{b}\, e^{jk_2(x-(t+l_1))} \qquad , t+l_1 \le x \le \Lambda \qquad \textbf{(3.3)}$$

$$H_Z = \frac{1}{\omega\mu}\left[k_2 \bar{a}\, e^{-jk_2(x-(t+l_1))} - k_2 \bar{b}\, e^{jk_2(x-(t+l_1))}\right] \qquad , t+l_1 \le x \le \Lambda \qquad \textbf{(3.4)}$$

$$k_i = \sqrt{(n_i k_0)^2 - \beta^2} \qquad , i = 1, 2. \qquad \textbf{(3.5)}$$

Here, n_1 and n_2 indicates the high and low refractive index layer, c the light velocity of vacuum. Using continuity of E_Y, H_Z at $x = t+l_1$:

$$a_1 e^{-jk_1 l_1} + b_1 e^{jk_1 l_1} = \bar{a} + \bar{b} \qquad \textbf{(3.6)}$$

$$\frac{k_1}{k_2} a_1 e^{-jk_1 l_1} - \frac{k_1}{k_2} b_1 e^{jk_1 l_1} = \bar{a} - \bar{b} \qquad \textbf{(3.7)}$$

Therefore:

$$2\bar{a} = \left(1+\frac{k_1}{k_2}\right) e^{-jk_1 l_1} a_1 + \left(1-\frac{k_1}{k_2}\right) e^{jk_1 l_1} b_1 \qquad \textbf{(3.8)}$$

$$2\bar{b} = \left(1 - \frac{k_1}{k_2}\right) e^{-jk_1 l_1} a_1 + \left(1 + \frac{k_1}{k_2}\right) e^{jk_1 l_1} b_1 \quad \textbf{(3.9)}$$

Next continuity condition is used for E_Y and H_Z at $x = \Lambda$. It should be noted that since x, $x+\Lambda$ are indistinguishable the fields should be identical except for a constant (Floquet Theorem).

E_Y and H_Z at $x = t^+$ are:

$$E_y(t^+) = a_1 + b_1 \quad \textbf{(3.10)}$$

$$H_Z(t^+) = \frac{1}{\omega\mu} k_1 (a_1 - b_1) \quad \textbf{(3.11)}$$

E_Y and H_Z at $x = \Lambda$ are:

$$E_y(\Lambda^+) = a_2 + b_2 \quad \textbf{(3.12)}$$

$$H_Z(\Lambda^+) = \frac{1}{\omega\mu} k_1 (a_2 - b_2) \quad \textbf{(3.13)}$$

As mentioned before, electric field at $x = \Lambda$ should be equal to electric field at $x = t^+$ times a Floquet constant

$$E_y(t^+)K = E_y(\Lambda^+) \quad \textbf{(3.14)}$$

$$H_Z(t^+)K = H_Z(\Lambda^+) \quad \textbf{(3.15)}$$

Using equation (3.10), (3.11) and equation (3.12), (3.13) upper equations are simplified as:

$$K(a_1 + b_1) = a_2 + b_2 \quad \textbf{(3.16)}$$

$$K(a_1 - b_1) = a_2 - b_2 \quad \textbf{(3.17)}$$

Using equation (3.16) and (3.17) in a matrix form:

$$K\begin{bmatrix} a_1 \\ b_1 \end{bmatrix} = \begin{bmatrix} a_2 \\ b_2 \end{bmatrix} \tag{3.18}$$

By using continuity condition at x = Λ^+ and x = Λ^-

$$E_Y\left(\Lambda^-\right) = \overline{a}\,e^{-jk_2l_2} + \overline{b}\,e^{jk_2l_2} = a_2 + b_2 = E_Y\left(\Lambda^+\right) \tag{3.19}$$

$$H_Z\left(\Lambda^-\right) = \frac{1}{\omega\mu}k_2\left[\overline{a}\,e^{-jk_2l_2} - \overline{b}\,e^{jk_2l_2}\right] = \frac{1}{\omega\mu}k_1\left(a_2 - b_2\right) \tag{3.20}$$

Equation (3.19) and (3.20) are simplified as:

$$\overline{a}\,e^{-jk_2l_2} + \overline{b}\,e^{jk_2l_2} = a_2 + b_2 \tag{3.21}$$

$$\frac{k_2}{k_1}\overline{a}\,e^{-jk_2l_2} - \frac{k_2}{k_1}\overline{b}\,e^{jk_2l_2} = a_2 - b_2 \tag{3.22}$$

Constant a_2 and b_2 are found from equations (3.21) and (3.22) as:

$$2a_2 = \left(1 + \frac{k_2}{k_1}\right)e^{-jk_2l_2}\overline{a} + \left(1 - \frac{k_2}{k_1}\right)e^{jk_2l_2}\overline{b} \tag{3.23}$$

$$2b_2 = \left(1 - \frac{k_2}{k_1}\right)e^{-jk_2l_2}\,\overline{a} + \left(1 + \frac{k_2}{k_1}\right)e^{jk_2l_2}\overline{b} \tag{3.24}$$

By using matrix formalism:

$$\begin{bmatrix} a_2 \\ b_2 \end{bmatrix} = \begin{bmatrix} \frac{1}{2}\left(1 + \frac{k_2}{k_1}\right)e^{-jk_2l_2} & \frac{1}{2}\left(1 - \frac{k_2}{k_1}\right)e^{jk_2l_2} \\ \frac{1}{2}\left(1 - \frac{k_2}{k_1}\right)e^{-jk_2l_2} & \frac{1}{2}\left(1 + \frac{k_2}{k_1}\right)e^{jk_2l_2} \end{bmatrix}\begin{bmatrix} \overline{a} \\ \overline{b} \end{bmatrix} \tag{3.25}$$

Substituting equation (3.8) and (3.9) into equation (3.25):

$$\begin{bmatrix} a_2 \\ b_2 \end{bmatrix} = \begin{bmatrix} A & B \\ B^* & A^* \end{bmatrix} \begin{bmatrix} a_1 \\ b_1 \end{bmatrix} \tag{3.26}$$

Constants A and B can be found by finding a_1 and b_1 in the form of the values $\bar{a}$ and $\bar{b}$ which can be found from equation (3.8) and (3.9). Than used these values into equation (3.25) and (3.26):

$$A = \frac{1}{2}\left(1+\frac{k_2}{k_1}\right)e^{-jk_2l_2} * \frac{1}{2}\left(1+\frac{k_1}{k_2}\right)e^{-jk_1l_1} + \frac{1}{2}\left(1-\frac{k_2}{k_1}\right)e^{jk_2l_2} * \frac{1}{2}\left(1-\frac{k_1}{k_2}\right)e^{-jk_1l_1} \tag{3.27}$$

The value of constant A can be simplified as:

$$A = e^{-jk_1l_1}\,\frac{1}{4}\left\{\left(2+\frac{k_2}{k_1}+\frac{k_1}{k_2}\right)e^{-jk_2l_2} + \left(2-\frac{k_2}{k_1}-\frac{k_1}{k_2}\right)e^{jk_2l_2}\right\} \tag{3.28}$$

$$A = e^{jk_1d_1}\left\{\cos(k_2l_2) - j\frac{1}{2}\left(\frac{k_2}{k_1}+\frac{k_1}{k_2}\right)\sin(k_2l_2)\right\} \tag{3.29}$$

Also value of B can be found as:

$$B = \frac{1}{2}\left(1+\frac{k_2}{k_1}\right)e^{-jk_2l_2} * \frac{1}{2}\left(1-\frac{k_1}{k_2}\right)e^{jk_1l_1} + \frac{1}{2}\left(1-\frac{k_2}{k_1}\right)e^{jk_2l_2} * \frac{1}{2}\left(1+\frac{k_1}{k_2}\right)e^{jk_1l_1} \tag{3.30}$$

$$B = e^{jk_1l_1}\,\frac{1}{4}\left\{\left(\frac{k_2}{k_1}-\frac{k_1}{k_2}\right)e^{-jk_2l_2} + \left(\frac{k_2}{k_1}-\frac{k_1}{k_2}\right)e^{jk_2l_2}\right\} \tag{3.31}$$

$$B = e^{jk_1l_1}\left\{-j\frac{1}{2}\left(\frac{k_2}{k_1}-\frac{k_1}{k_2}\right)\sin(k_2l_2)\right\} \tag{3.32}$$

It should be noted that determinant (ABCD) = AA^*-BB^* = 1.

$$AA^* - BB^* = \cos^2(k_2l_2) + \frac{1}{4}\left(\frac{k_2}{k_1}+\frac{k_1}{k_2}\right)^2\sin^2(k_2l_2) - \frac{1}{4}\left(\frac{k_2}{k_1}-\frac{k_1}{k_2}\right)^2\sin^2(k_2l_2) \tag{3.33}$$

$$AA^* - BB^* = \cos^2(k_2 l_2) + \sin^2(k_2 l_2)\left[\frac{1}{4}\frac{(k_2^2 + k_1^2) - (k_2^2 - k_1^2)}{k_2^2 k_1^2}\right] = 1 \qquad \textbf{(3.34)}$$

To determine the eigenvalue K:

$$\begin{bmatrix} a_2 \\ b_2 \end{bmatrix} = \begin{bmatrix} A & B \\ B^* & A^* \end{bmatrix}\begin{bmatrix} a_1 \\ b_1 \end{bmatrix} = K\begin{bmatrix} a_1 \\ b_1 \end{bmatrix} \qquad \textbf{(3.35)}$$

$$\begin{bmatrix} A-K & B \\ B^* & A^*-K \end{bmatrix}\begin{bmatrix} a_1 \\ b_1 \end{bmatrix} = 0 \qquad \textbf{(3.36)}$$

Equation (3.36) is equal to zero if;

$$\det\begin{vmatrix} A-K & B \\ B^* & A^*-K \end{vmatrix} = 0 \qquad \textbf{(3.37)}$$

$$|A|^2 + K^2 - |B|^2 + (A^* - A)K = 0 \qquad \textbf{(3.38)}$$

$|A|^2 - |B|^2 = 1$ from equation(3.34). So equation (3.38) can be simplified to

$$K^2 - (A - A^*)K + 1 = 0 \qquad \textbf{(3.39)}$$

$$K_j = \frac{1}{2}\left[(A - A^*) \pm \sqrt{(A - A^*)^2 - 4}\right] \qquad \text{j=1, 2} \qquad \textbf{(3.40)}$$

The upper (lower) sign in the double sign notation corresponds to j = 1 (2). For Bragg waveguides real values of K is interested (which characterized a stop band of the periodic structure) and choose the one which is less than one in order to ensure proper decay as x → ∞.

$$(A - K_j)a_1 = -Bb_1 \Rightarrow a_1 = \frac{-B}{(A - K_j)}b_1 \qquad \textbf{(3.41)}$$

$$B^* a_1 = -(A^* - K_j)b_1 \Rightarrow a_1 = \frac{-(A^* - K_j)}{B^*}b_1 \qquad \textbf{(3.42)}$$

With equation (3.41) and (3.42) a relation between a_1 and b_1 is found. This relation is used in the boundary condition at x = t to obtain the modal eigenvalues of the Bragg waveguides.

At $0 \leq x \leq t$:

$$E_Y = E_0 \sin(k_c x) \tag{3.43}$$

$$H_z = j\frac{k_g}{\omega\mu} E_0 \cos(k_c x) \tag{3.44}$$

$$k_c = \sqrt{(n_c k_0)^2 - \beta^2} \tag{3.45}$$

Here, $k_0 = \omega / c = 2\pi / \lambda_0$ indicates the wavenumber of vacuum, c the light velocity of vacuum, λ_0 the vacuum wavelength and μ the dielectric permeability of vacuum. In equation (3.1) and equation (3.2) the fields' expression is given at $t \leq x \leq t+l_1$. If the boundary condition is applied at x = t:

$$E_0 \sin(k_c t) = a_1 + b_1 \tag{3.46}$$

$$j\frac{k_c}{k_1} E_0 \cos(k_c t) = a_1 - b_1 \tag{3.47}$$

$$jk_c \cot(k_c t) = k_1 \frac{a_1 - b_1}{a_1 + b_1} \tag{3.48}$$

Using the relation between a_1 and b_1 equation (3.41):

$$-jk_c \cot(k_c t) = k_1 \frac{K_j - A - B}{K_j - A + B} \tag{3.49}$$

which is the equation for finding propagation constant of odd TE modes.

It is straightforward to show that the formulation given above applies directly also for even symmetric TE modes provided that the eigenvalue equation given in equation (3.49) is modified as:

$$jk_c \tan(k_c t) = k_1 \frac{K_j - A - B}{K_j - A + B} \qquad \textbf{(3.50)}$$

On the other hand TM modes of planar Bragg structures can also be obtained in a similar manner. In this case one would have for odd symmetric TM modes:

$$\frac{jk_g n_1^{\,2}}{n_c^2 k_1} \tan(k_c t) = \frac{K_j - A - B}{K_j - A + B} \qquad \textbf{(3.51)}$$

As noted for the TE case the formulation for even TM mode is identical except that the eigenvalue equation given in equation (3.51) has to be modified as:

$$-\frac{jk_g n_1^{\,2}}{n_c^2 k_1} \cot(k_c t) = \frac{K_j - A - B}{K_j - A + B} \qquad \textbf{(3.52)}$$

3.2 Multilayered Structures

It may be of interest to generalize the formulations given for 2-layered structures to the case of multilayered structures. For illustrating the generalization process the derivation of formulations for a 3-layered structure as shown in figure (3.2) will be considered in this subsection.

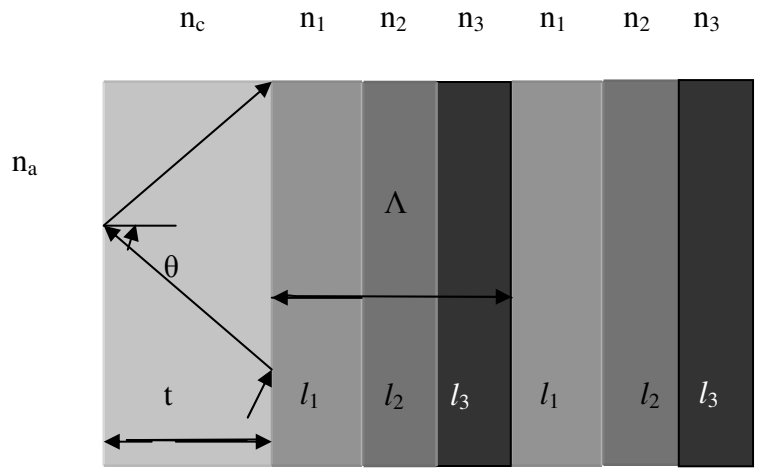

Figure 3.2 : A Bragg reflection (slab) dielectric waveguide as 3-layered structure.

Planar Bragg waveguide consists of a guiding region of thickness 2t and refractive index n_c, imbedded on both sides in symmetrical cladding regions with period $\Lambda = l_1+l_2+l_3$.

$$E_Y = a_1 e^{-jk_1(x-t)} + b_1 e^{jk_1(x-t)} \qquad , t \le x \le t+l_1 \qquad \textbf{(3.53)}$$

$$H_Z = \frac{1}{\omega\mu}\left[k_1 a_1 e^{-jk_1(x-t)} - k_1 b_1 e^{jk_1(x-t)}\right] \qquad , t \le x \le t+l_1 \qquad \textbf{(3.54)}$$

$$E_Y = \bar{a}\, e^{-jk_2(x-(t+d_1))} + \bar{b}\, e^{jk_2(x-(t+d_1))} \qquad , t+l_1 \le x \le t+l1+l_2 \qquad \textbf{(3.55)}$$

$$H_Z = \frac{1}{\omega\mu}\left[k_2 \bar{a}\, e^{-jk_2(x-(t+d_1))} - k_2 \bar{b}\, e^{jk_2(x-(t+d_1))}\right] \qquad , t+l_1 \le x \le t+l1+l_2 \qquad \textbf{(3.56)}$$

$$E_Y = \tilde{a}\, e^{-jk_3(x-(t+d_1+d_2))} + \tilde{b}\, e^{jk_3(x-(t+d_1+d_2))} \qquad , t+l_1+l_2 \le x \le \Lambda \qquad \textbf{(3.57)}$$

$$H_Z = \frac{1}{\omega\mu}\left[k_3 \tilde{a}\, e^{-jk_3(x-(t+d_1+d_2))} - k_3 \tilde{b}\, e^{jk_3(x-(t+d_1+d_2))}\right] \qquad , t+l_1+l_2 \le x \le \Lambda \qquad \textbf{(3.58)}$$

Using continuity of E_Y, H_Z at $x = t+l_1$:

$$a_1 e^{-jk_1 d_1} + b_1 e^{jk_1 d_1} = \bar{a} + \bar{b} \qquad \textbf{(3.59)}$$

$$\frac{k_1}{k_2} a_1 e^{-jk_1 d_1} - \frac{k_1}{k_2} b_1 e^{jk_1 d_1} = \overline{a} - \overline{b} \tag{3.60}$$

Therefore:

$$2\overline{a} = \left(1+\frac{k_1}{k_2}\right) e^{-jk_1 d_1} a_1 + \left(1-\frac{k_1}{k_2}\right) e^{jk_1 d_1} b_1 \tag{3.61}$$

$$2\overline{b} = \left(1-\frac{k_1}{k_2}\right) e^{-jk_1 d_1} a_1 + \left(1+\frac{k_1}{k_2}\right) e^{jk_1 d_1} b_1 \tag{3.62}$$

In matrix formalism these equations equal to

$$\begin{bmatrix} \overline{a} \\ \overline{b} \end{bmatrix} = \begin{bmatrix} \frac{1}{2}\left(1+\frac{k_1}{k_2}\right) e^{-jk_1 d_1} & \frac{1}{2}\left(1-\frac{k_1}{k_2}\right) e^{jk_1 d_1} \\ \frac{1}{2}\left(1-\frac{k_1}{k_2}\right) e^{-jk_1 d_1} & \frac{1}{2}\left(1+\frac{k_1}{k_2}\right) e^{jk_1 d_1} \end{bmatrix} \begin{bmatrix} a_1 \\ b_1 \end{bmatrix} \tag{3.63}$$

Using continuity of E_Y, H_Z at $x = t+l_1+l_2$:

$$\overline{a} e^{-jk_2 d_2} + \overline{b} e^{jk_2 d_2} = \tilde{a} + \tilde{b} \tag{3.64}$$

$$\frac{k_2}{k_3} \overline{a} e^{-jk_2 d_2} - \frac{k_2}{k_3} \overline{b} e^{jk_2 d_2} = \tilde{a} - \tilde{b} \tag{3.65}$$

Coefficients are related each other by:

$$\begin{bmatrix} \tilde{a} \\ \tilde{b} \end{bmatrix} = \begin{bmatrix} \frac{1}{2}\left(1+\frac{k_2}{k_3}\right) e^{-jk_2 d_2} & \frac{1}{2}\left(1-\frac{k_2}{k_3}\right) e^{jk_2 d_2} \\ \frac{1}{2}\left(1-\frac{k_2}{k_3}\right) e^{-jk_2 d_2} & \frac{1}{2}\left(1+\frac{k_2}{k_3}\right) e^{jk_2 d_2} \end{bmatrix} \begin{bmatrix} \overline{a} \\ \overline{b} \end{bmatrix} \tag{3.66}$$

Next continuity condition is used for E_Y and H_Z at $x = \Lambda$. It should be noted that since x, $x+\Lambda$ are indistinguishable the fields should be identical except for a constant (Floquet Theorem).

E_Y and H_Z at $x = t^+$ are:

$$E_y\left(t^+\right) = a_1 + b_1 \tag{3.67}$$

$$H_Z\left(t^+\right) = \frac{1}{\omega\mu} k_1\left(a_1 - b_1\right) \tag{3.68}$$

E_Y and H_Z at $x = \Lambda$ are:

$$E_y\left(\Lambda^+\right) = a_2 + b_2 \tag{3.69}$$

$$H_Z\left(\Lambda^+\right) = \frac{1}{\omega\mu} k_1\left(a_2 - b_2\right) \tag{3.70}$$

As mentioned before, electric field at $x = \Lambda$ should be equal to electric field at $x = t^+$ times a Floquet constant

$$E_y\left(t^+\right)K = E_y\left(\Lambda^+\right) \tag{3.71}$$

$$H_Z\left(t^+\right)K = H_Z\left(\Lambda^+\right) \tag{3.72}$$

Using equation (3.69), (3.70) and equation (3.71), (3.72) upper equations are simplified as:

$$K\left(a_1 + b_1\right) = a_2 + b_2 \tag{3.73}$$

$$K\left(a_1 - b_1\right) = a_2 - b_2 \tag{3.74}$$

Using equation (3.73) and (3.74) in a matrix form:

$$K\begin{bmatrix} a_1 \\ b_1 \end{bmatrix} = \begin{bmatrix} a_2 \\ b_2 \end{bmatrix} \tag{3.75}$$

By using continuity condition at x = Λ^+ and x = Λ^-

$$E_Y\left(\Lambda^-\right) = \tilde{a}\,e^{-jk_3d_3} + \tilde{b}\,e^{jk_3d_3} = a_2 + b_2 = E_Y\left(\Lambda^+\right) \tag{3.76}$$

$$H_Z\left(\Lambda^-\right) = \frac{1}{\omega\mu}k_3\left[\tilde{a}\,e^{-jk_3d_3} - \tilde{b}\,e^{jk_3d_3}\right] = \frac{1}{\omega\mu}k_1\left(a_2 - b_2\right) \tag{3.77}$$

Equation (3.76) and (3.77) are simplified as:

$$\tilde{a}\,e^{-jk_3d_3} + \tilde{b}\,e^{jk_3d_3} = a_2 + b_2 \tag{3.78}$$

$$\frac{k_3}{k_1}\tilde{a}\,e^{-jk_3d_3} - \frac{k_3}{k_1}\tilde{b}\,e^{jk_3d_3} = a_2 - b_2 \tag{3.79}$$

Constant a_2 and b_2 are found from equations (3.78) and (3.79) as:

$$2a_2 = \left(1 + \frac{k_3}{k_1}\right)e^{-jk_3d_3}\tilde{a} + \left(1 - \frac{k_3}{k_1}\right)e^{jk_3d_3}\tilde{b} \tag{3.80}$$

$$2b_2 = \left(1 - \frac{k_3}{k_1}\right)e^{-jk_3d_3}\,\tilde{a} + \left(1 + \frac{k_3}{k_1}\right)e^{jk_3d_3}\tilde{b} \tag{3.81}$$

By using matrix formalism:

$$\begin{bmatrix} a_2 \\ b_2 \end{bmatrix} = \begin{bmatrix} \frac{1}{2}\left(1 + \frac{k_3}{k_1}\right)e^{-jk_3d_3} & \frac{1}{2}\left(1 - \frac{k_3}{k_1}\right)e^{jk_3d_3} \\ \frac{1}{2}\left(1 - \frac{k_3}{k_1}\right)e^{-jk_3d_3} & \frac{1}{2}\left(1 + \frac{k_3}{k_1}\right)e^{jk_3d_3} \end{bmatrix}\begin{bmatrix} \tilde{a} \\ \tilde{b} \end{bmatrix} \tag{3.82}$$

Substituting equation (3.63) and (3.66) into equation (3.82):

$$\begin{bmatrix} a_2 \\ b_2 \end{bmatrix} = \begin{bmatrix} A & B \\ B^* & A^* \end{bmatrix} \begin{bmatrix} a_1 \\ b_1 \end{bmatrix} \tag{3.83}$$

Constants A and B can be found by finding $\tilde{a}$ and $\tilde{b}$ in the form of the values $\bar{a}$ and $\bar{b}$ which can be found from equation (3.66) and then by finding a_1 and b_1 in the form of $\bar{a}$ and $\bar{b}$ from equation (3.66). Then used these values into equation (3.82) and (3.83):

$$\begin{aligned} A = \frac{1}{2}\Big(\frac{1}{4}\Big(1+\frac{k_3}{k_1}\Big)\exp(-jk_3d_3)\Big(1+\frac{k_2}{k_3}\Big)\exp(-jk_2d_2)+\frac{1}{4}\Big(1-\frac{k_3}{k_1}\Big)\exp(jk_3d_3)\Big(1-\frac{k_2}{k_3}\Big) \\ \exp(-jk_2d_2)\Big)\Big(1+\frac{k_1}{k_2}\Big)\exp(-jk_1d_1)+\frac{1}{2}\Big(\frac{1}{4}\Big(1+\frac{k_3}{k_1}\Big)\exp(-jk_3d_3)\Big(1-\frac{k_2}{k_3}\Big)\exp(jk_2d_2) \\ +\frac{1}{4}\Big(1-\frac{k_3}{k_1}\Big)\exp(jk_3d_3)\Big(1+\frac{k_2}{k_3}\Big)\exp(jk_2d_2)\Big)+\Big(1-\frac{k_1}{k_2}\Big)\exp(-jk_1d_1) \end{aligned} \tag{3.84}$$

Also value of B can be found as:

$$\begin{aligned} B = \frac{1}{2}\Big(\frac{1}{4}\Big(1+\frac{k_3}{k_1}\Big)\exp(-jk_3d_3)\Big(1+\frac{k_2}{k_3}\Big)\exp(-jk_2d_2)+\frac{1}{4}\Big(1-\frac{k_3}{k_1}\Big)\exp(jk_3d_3)\Big(1-\frac{k_2}{k_3}\Big) \\ \exp(-jk_2d_2)\Big)\Big(1-\frac{k_1}{k_2}\Big)\exp(-jk_1d_1)+\frac{1}{2}\Big(\frac{1}{4}\Big(1+\frac{k_3}{k_1}\Big)\exp(-jk_3d_3)\Big(1-\frac{k_2}{k_3}\Big)\exp(jk_2d_2) \\ +\frac{1}{4}\Big(1-\frac{k_3}{k_1}\Big)\exp(jk_3d_3)\Big(1+\frac{k_2}{k_3}\Big)\exp(jk_2d_2)\Big)+\Big(1+\frac{k_1}{k_2}\Big)\exp(-jk_1d_1) \end{aligned} \tag{3.85}$$

It should be noted that determinant (ABCD) = AA^*-BB^* = 1.

To determine the eigenvalue K:

$$\begin{bmatrix} a_2 \\ b_2 \end{bmatrix} = \begin{bmatrix} A & B \\ B^* & A^* \end{bmatrix} \begin{bmatrix} a_1 \\ b_1 \end{bmatrix} = K \begin{bmatrix} a_1 \\ b_1 \end{bmatrix} \tag{3.86}$$

$$\begin{bmatrix} A-K & B \\ B^* & A^*-K \end{bmatrix} \begin{bmatrix} a_1 \\ b_1 \end{bmatrix} = 0 \tag{3.87}$$

Equation (3.87) is equal to zero if;

$$\det\begin{vmatrix} A-K & B \\ B^* & A^*-K \end{vmatrix} = 0 \qquad \textbf{(3.88)}$$

$$|A|^2 + K^2 - |B|^2 + (A^* - A)K = 0 \qquad \textbf{(3.89)}$$

$|A|^2 - |B|^2 = 1$ from equation(3.34). So equation (3.38) can be simplified to

$$K^2 - (A - A^*)K + 1 = 0 \qquad \textbf{(3.90)}$$

$$K_j = \frac{1}{2}\left[(A - A^*) \pm \sqrt{(A - A^*)^2 - 4}\right] \qquad \text{j=1, 2} \qquad \textbf{(3.91)}$$

The upper (lower) sign in the double sign notation corresponds to j = 1 (2). For Bragg waveguides real values of K is interested (which characterized a stop band of the periodic structure) and choose the one which is less than one in order to ensure proper decay as x → ∞.

$$(A - K_j)a_1 = -Bb_1 \Rightarrow a_1 = \frac{-B}{(A - K_j)}b_1 \qquad \textbf{(3.92)}$$

$$B^* a_1 = -(A^* - K_j)b_1 \Rightarrow a_1 = \frac{-(A^* - K_j)}{B^*}b_1 \qquad \textbf{(3.93)}$$

With equation (3.41) and (3.42) a relation between a_1 and b_1 is found. This relation is used in the boundary condition at x = t to obtain the modal eigenvalues of the Bragg waveguides.

At $0 \le x \le t$:

$$E_Y = E_0 \sin(k_c x) \qquad \textbf{(3.94)}$$

$$H_z = j\frac{k_g}{\omega\mu}E_0 \cos(k_c x) \qquad \textbf{(3.95)}$$

$$k_c = \sqrt{(n_c k_0)^2 - \beta^2} \qquad \textbf{(3.96)}$$

Here, $k_0 = \omega / c = 2\pi / \lambda_0$ indicates the wavenumber of vacuum, c the light velocity of vacuum, λ_0 the vacuum wavelength and μ the dielectric permeability of vacuum. In equation (3.1) and equation (3.2) the fields' expression is given at $t \leq x \leq t+l_1$. If the boundary condition is applied at x = t:

$$E_0 \sin(k_c t) = a_1 + b_1 \tag{3.97}$$

$$j\frac{k_c}{k_1} E_0 \cos(k_c t) = a_1 - b_1 \tag{3.98}$$

$$jk_c \cot(k_c t) = k_1 \frac{a_1 - b_1}{a_1 + b_1} \tag{3.99}$$

Using the relation between a_1 and b_1 equation (3.41):

$$-jk_c \cot(k_c t) = k_1 \frac{K_j - A - B}{K_j - A + B} \tag{3.100}$$

which is the equation for finding propagation constant of odd TE modes.

3.3 Numerical Results

For the purpose of verification of the formulations and of their coding first a special problem is considered for which numerical solutions are given in the literature [5]. The particular problem to be considered is the determination of the transverse field distribution of the fundamental mode of a typical Bragg reflection waveguide figure (3.2) with following parameters: $n_c = 1.0$, $n_2 = 3.38$, $n_1 = 2.89$, $\lambda = 1.15\mu$, $l_1 = l_2 = 0.5\Lambda = 0.1\mu$m. For the above parameters the Bloch constant (K) is found from equation (3.40) as -0.8949 for even modes For the first even mode the eigenvalue equation in (3.49) yields $\beta/k_0 = 0.93$ and t = 1.4975 μm.

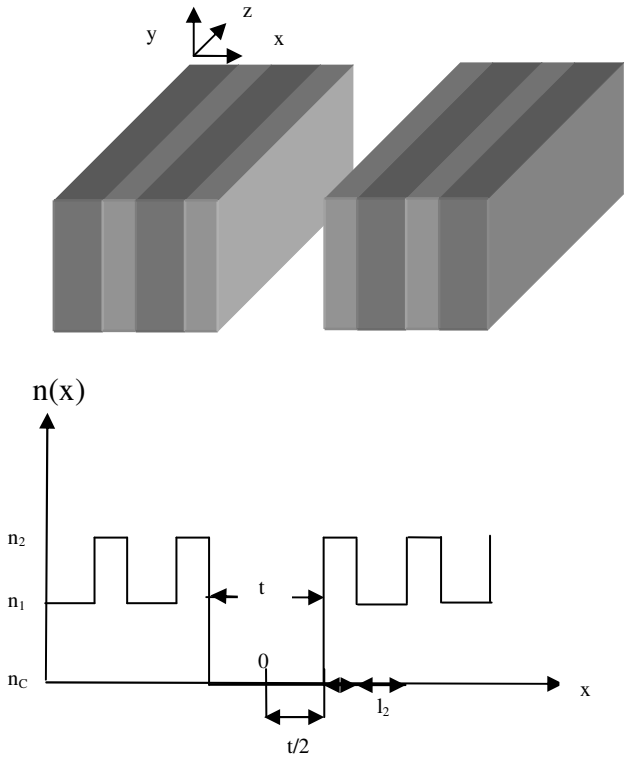

Figure 3.3 : A typical Bragg reflection waveguide.

Transverse field distributions of the fundamental even mode is plotted in figure (3.3). From this figure it is clear that substantial part of the field is guided within the air core and it decays in an exponential manner as one proceeds into the cladding region. It is to be noted that the field variation given in figure (3.3) exhibits identical features with the solutions reported in the literature (see figure 3 in [5]). However, there is one interesting difference since we have obtained a negative value of the Bloch constant K only the amplitude of our solution is periodic in Λ, i.e. the fields are related as $U(x) = U(x+\Lambda)$.

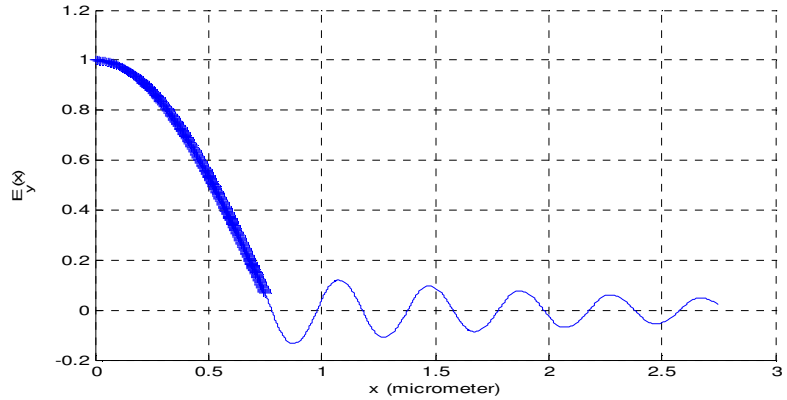

Figure 3.4 : First even TE mode(a.u.) , bold region shows the core thickness.

It should be noted that the eigenvalue equation (3.49) accepts a set of different solutions with identical field variations in certain regions for different values of the thickness of the core region, t defined as:

$$t_n = t_0 + n\pi / k_c \qquad \textbf{(3.101)}$$

In figure (3.4) the variation for t is plotted together with that corresponding to t_0 and given in figure (3.3). As expected the behaviour of the field is identical in common portions of the core region and also in the cladding.

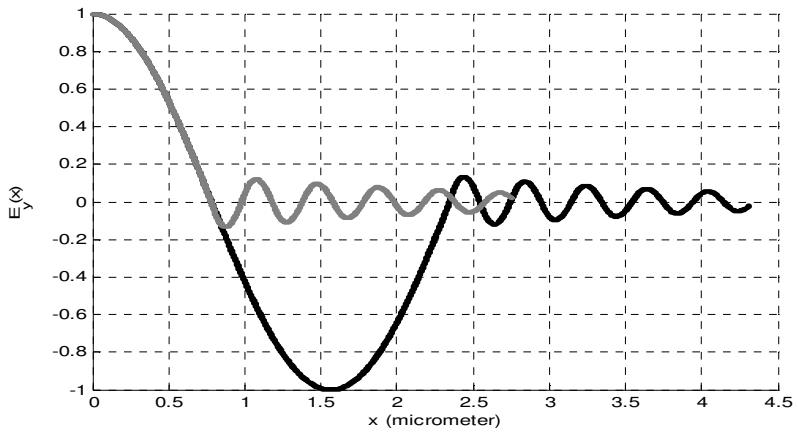

Figure 3.5 : First even TE mode(a.u.), black one correspons to $t_n = t_0+2\pi/k_c$,the other is $t_n = t_0$

As a further example we use the parametres, which correspond to those used for determining the variation of the dominant TE mode in Bragg fiber using asymptotical approach (see figure 4.4). In this case: $n_c = 1$, $\rho_1 = 1$ μm, $n_1 = 3.0$, $l_1 = 0.130$ μm, $n_2 = 1.5$ and $l_2 = 0.265$ μm, $\lambda = 1.55$ and the variation of E_Y field component (which corresponds to E_θ given in figure (4.4)) is shown in figure (3.5). When the parameters are identical it should be noted that, the variation of the field in the planar Bragg structure and in the Bragg fiber exhibit similar features.

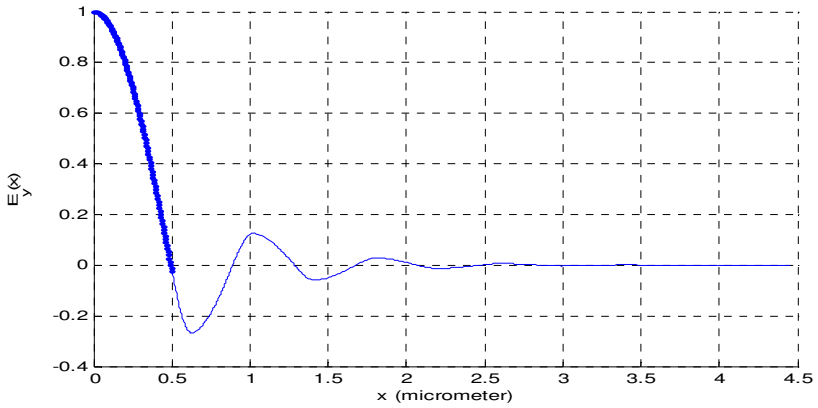

Figure 3.6 : First even TE mode(a.u.) , bold region shows the core thickness.

In figure (3.6) we present a TM mode example. In this case parameters are: $n_c = 1.0$, $n_2 = 3.38$, $n_1 = 2.289$, $\lambda = 1.15$μm, $l_1 = l_2 = 0.5\Lambda = 0.1$μm.

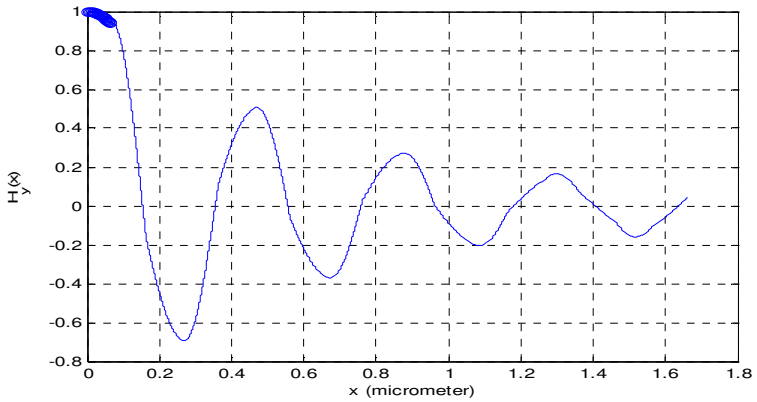

Figure 3.7 : First odd TM mode(a.u.) , bold region shows the core thickness.

In connection with this figure(3.6) we note that as expected the slope of H_Y is discontinuous at interfaces, bold region shows the core thickness.

For the purpose of verification of the formulations and of their coding of three-layered planar Bragg structure a special problem is considered for which numerical solutions are given in the literature [5] for two-layered planar Bragg structure. The particular problem to be considered is the determination of the transverse field distribution of the fundamental mode of a typical Bragg reflection waveguide with following parameters: $n_c = 1.0$, $n_1 = 3.38$, $n_2 = 2.89$, $n_3 = 2.89$, $\lambda = 1.15\mu m$, $l_1 = 0.5\Lambda = 0.1\mu m$, $l_2 = l_3 = 0.25\Lambda = 0.05\mu m$. For the above parameters the Bloch constant (K) is found from equation (3.91) as -0.89487 for even modes For the first even mode the eigenvalue equation in (3.100) yields $\beta/k_0 = 0.93$ and $t = 1.4975\ \mu m$. It should be noted that when the refractive index and the thickness of the third layer is identical with the second layer and other parameters are same with the two-layered planar Bragg structure of the first example, the variation of the field is similar with the two-layered planar Bragg structure.

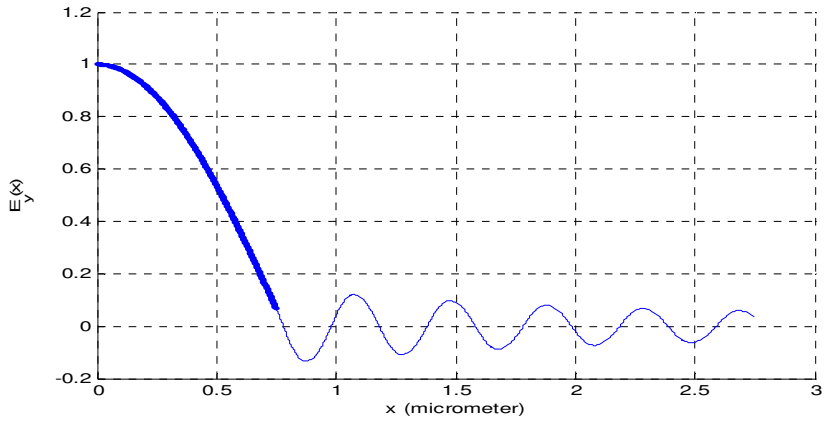

Figure 3.8 : First even TE mode(a.u.) of three-layered planar Bragg structure, bold region shows the core thickness.

4. ASYMPTOTIC ANALYSIS OF BRAGG FIBER

In this chapter the (simple) asymptotic analysis of Bragg fiber is investigated. We refer to this approach as simple asymptotics since only the fields in the core region are retained in exact form and fields in all cladding regions are treated asymptotically. In the next chapter the extended version is presented which will be called asymptotic matrix theory of Bragg fiber, wherein the fields in the core as well as in a predetermined number of cladding regions are retained in exact form and asymptotic approach is applied for the remaining cladding layers. For guided modes the temporal and the z dependence can be factored out as exp (i(βz-ωt)) and the azimuthal dependence as cos($l\theta$) or sin($l\theta$), hence the axial field component can be written as:

At $r \le r_c$:

$$E_Z = E_0 J_l(k_C r)\sin(l\theta) \tag{4.1}$$

$$H_Z = H_0 J_l(k_C r)\cos(l\theta) \tag{4.2}$$

$$k_C = \sqrt{(n_C k_0)^2 - \beta^2} \tag{4.3}$$

At $r_c \le r \le r_c+l1$:

$$E_Z = [A_1 J_l(k_1 r) + B_1 Y_l(k_1 r)]\sin(l\theta) \tag{4.4}$$

$$H_Z = [C_1 J_l(k_1 r) + D_1 Y_l(k_1 r)]\cos(l\theta) \tag{4.5}$$

At $r_c+l1 \le r \le r_c+\Lambda$:

$$E_Z = [A_1' J_l(k_2 r) + B_1' Y_l(k_2 r)]\sin(l\theta) \tag{4.6}$$

$$H_Z = [C_1' J_l(k_2 r) + D_1' Y_l(k_2 r)]\cos(l\theta) \tag{4.7}$$

$$k_i = \sqrt{(n_i k_0)^2 - \beta^2} \qquad , \ i = 1, 2 \qquad \textbf{(4.8)}$$

Here, $k_0 = \omega / c = 2\pi / \lambda_0$ indicates the wave number of vacuum, c the light velocity of vacuum, λ_0 the vacuum wavelength and n_1, n_2 indicates the high and low refractive index layer of the structure. Dual solution can be written by exchanging sin and cos terms above. Fields components in the cladding layer $r > r_g+\Lambda$ are in similar form with different amplitude factors.

Other field components are obtained as:

$$\vec{E}_t = \frac{-j\beta}{k^2}\left(\nabla_t E_Z + \frac{w\mu}{\beta}\nabla_t H_Z \times \vec{u}_Z\right) \qquad \textbf{(4.9)}$$

$$\vec{H}_t = \frac{-j\beta}{k^2}\left(\nabla_t H_Z + \frac{w\varepsilon n^2}{\beta}\nabla_t H_Z \times \vec{u}_Z\right) \qquad \textbf{(4.10)}$$

At this point, it would be appropriate to discuss briefly the difficulties involved in determining exact solutions of the Bragg fiber problem. We note that one has radially inward and outward propagating waves both in the core and cladding regions one has for the transverse propagating constants k_0, k_1, $k_2 > 0$. As shown below the fields are described by 2+4+4 = 10 coefficients which is incompatible with the 8 equations resulting from continuity at the interfaces.

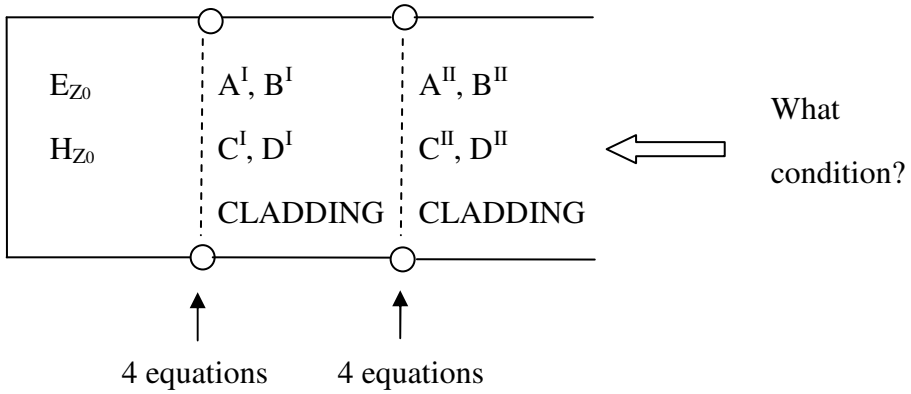

Figure 4.1 : Schematic of the problem between coefficients and equations equality.

In conventional fiber we have 2 coefficients in the last cladding layer (radiation condition) and hence a computable system of equations. However, in Bragg Fibers, two more equations are needed. Thus, it is needed to impose another condition. In periodic planar structures such a condition was obtained using Floquet theorem. However, Bragg Fiber is not periodic structure and Floquet theorem is not applicable.

To overcome this difficulty Yeh and Yariv have [5] proposed that the coefficients in each layer be chosen on such a way that the outward radial flux through the layer is minimized and that corresponds to a stop band of a periodic structure. The implementation of this approach is very difficult. Because of this there are some methods for solving the problem. One of them is asymptotic analysis method.

Cylindrical coordinate system (r, θ, z) is used to analyze the property of optical fibers with cylindrically symmetric index distribution [10]. It is assumed that the fiber structure is uniform along the optical propagation direction, z and assume that electromagnetic field components have a spatio-temporal factor exp [i(ωt-βz)].

It is clear that the arguments of Bessel functions will grow (with r) as one moves away from the core region and hence it becomes possible to use asymptotic approximation for Bessel functions without degrading accuracy.

It is noted that for fixed n and large x:

$$J_n(x) = \sqrt{\frac{2}{\pi x}} \cos\left(x - \frac{n\pi}{2} - \frac{\pi}{4} \right) \tag{4.11}$$

$$Y_n(x) = \sqrt{\frac{2}{\pi x}} \sin\left(x - \frac{n\pi}{2} - \frac{\pi}{4} \right) \tag{4.12}$$

Thus:

$$E_Z = \sqrt{\frac{2}{\pi}} \frac{1}{\sqrt{kr}} \left\{ \begin{array}{l} \frac{\exp(-jn\pi/2)\exp(-j\pi/4)}{2}(A + jB)e^{jkr} + \\ \frac{\exp(-jn\pi/2)\exp(-j\pi/4)}{2}(A - jB)e^{-jkr} \end{array} \right\} \cos n\phi \tag{4.13}$$

Omitting the cos (nØ) term which is irrelevant in determining modal fields and defines:

$$\bar{a} = \frac{1}{\sqrt{2\pi}} \exp(-jn\pi/2)\exp(-j\pi/4)(A - jB) \quad \textbf{(4.14)}$$

$$\bar{b} = \frac{1}{\sqrt{2\pi}} \exp(-jn\pi/2)\exp(-j\pi/4)(A + jB) \quad \textbf{(4.15)}$$

So the E_Z becomes:

$$E_Z = \frac{\bar{a}e^{-jkr} + \bar{b}e^{jkr}}{\sqrt{kr}} \quad \textbf{(4.16)}$$

Similarly at r+Δr:

$$E_Z = \frac{\bar{a}e^{-jkr}e^{-jk\Delta r} + \bar{b}e^{jkr}e^{jk\Delta r}}{\sqrt{k(r+\Delta r)}} \quad \textbf{(4.17)}$$

Setting $r = r_0$ and $\bar{a}e^{-jkr_0} = a$, $\bar{b}e^{-jkr_0} = b$, at $r_0 < r < r_1 = r_0 + \Delta r$:

$$E_Z = \frac{a\exp(-jk(r-r_0)) + b\exp(jk(r-r_0))}{\sqrt{kr}} \quad \textbf{(4.18)}$$

To demonstrate this approach TE modes are considered (n = 0) and assuming asymptotic approach can be used in all layers except for the first one which is low-index core region.

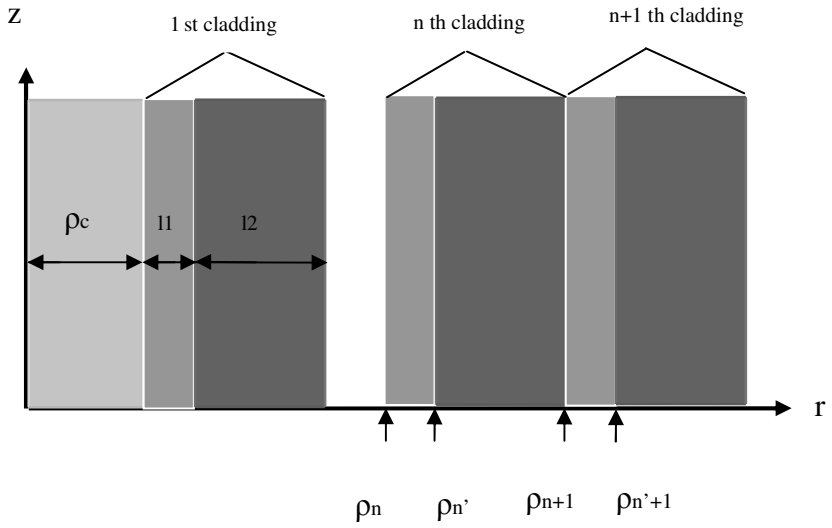

Figure 4.2 : Schematic of the r-z cross section of a Bragg fiber.

$$H_z = \frac{a_1 \exp[-ik_1 r] + b_1 \exp[ik_1 r]}{\sqrt{k_1 (r+\rho_1)}} \qquad , \rho_1 < r < \rho_1 + l_1 \qquad \textbf{(4.19)}$$

$$E_\theta = \frac{\omega\mu}{k_1} \frac{a_1 \exp[-ik_1 r] - b_1 \exp[ik_1 r]}{\sqrt{k_1 (r+\rho_1)}} \qquad , \rho_1 < r < \rho_1 + l_1 \qquad \textbf{(4.20)}$$

$$H_z = \frac{\bar{a} \exp[-ik_2 (r-l_1)] + \bar{b} \exp[ik_2 (r-l_1)]}{\sqrt{k_2 (r+\rho_1)}} \qquad , \rho_1 + l_1 < r < \rho_1 + l_1 + l_2 \qquad \textbf{(4.21)}$$

$$E_\theta = \frac{\omega\mu}{k_2} \frac{\bar{a} \exp[-ik_2 (r-l_1)] + \bar{b} \exp[ik_2 (r-l_1)]}{\sqrt{k_2 (r+\rho_1)}} \qquad , \rho_1 + l_1 < r < \rho_1 + l_1 + l_2 \qquad \textbf{(4.22)}$$

From the continuity condition at r = l_1:

$$[a_1 \exp(-jk_1 l_1) + b_1 \exp(jk_1 l_1)] \sqrt{\frac{k_2}{k_1}} = \bar{a} + \bar{b} \qquad \textbf{(4.23)}$$

$$[a_1 \exp(-jk_1 l_1) - b_1 \exp(jk_1 l_1)] \frac{k_2}{k_1} \sqrt{\frac{k_2}{k_1}} = \bar{a} - \bar{b} \qquad \textbf{(4.24)}$$

$$\bar{a} = \frac{1}{2}\sqrt{\frac{k_2}{k_1}}\left[\left(1+\frac{k_2}{k_1}\right)e^{-jk_1l_1}a_1 + \left(1-\frac{k_2}{k_1}\right)e^{jk_1l_1}b_1\right] \quad \textbf{(4.25)}$$

$$\bar{b} = \frac{1}{2}\sqrt{\frac{k_2}{k_1}}\left[\left(1-\frac{k_2}{k_1}\right)e^{-jk_1l_1}a_1 + \left(1+\frac{k_2}{k_1}\right)e^{jk_1l_1}b_1\right] \quad \textbf{(4.26)}$$

Also using the boundary conditions at r = l_1+l_2:

$$a_2 + b_2 = \left[\bar{a}\exp(-jk_2l_2) + \bar{b}\exp(jk_2l_2)\right]\sqrt{\frac{k_1}{k_2}} \quad \textbf{(4.27)}$$

$$a_2 - b_2 = \left[\bar{a}\exp(-jk_2l_2) + \bar{b}\exp(jk_2l_2)\right]\frac{k_1}{k_2}\sqrt{\frac{k_1}{k_2}} \quad \textbf{(4.28)}$$

Thus similar to the planar case when combining these results:

$$\begin{bmatrix} a_2 \\ b_2 \end{bmatrix} = \begin{bmatrix} A & B \\ B^* & A^* \end{bmatrix}\begin{bmatrix} a_1 \\ b_1 \end{bmatrix} \quad \textbf{(4.29)}$$

All deviations found for planar case are remain valid. In particular the relation between a_1 and b_1 is:

$$a_1 = \frac{-B}{A-K_j}b_1 \quad \textbf{(4.30)}$$

For finding eigenvalue equation boundary condition at r = ρ_1 is used:

$$AJ_0(k_C\rho_1) = \frac{1}{\sqrt{k_1\rho_1}}(a_1+b_1) = \frac{1}{\sqrt{k_1\rho_1}}\left(1-\frac{B}{A-K_j}\right)b_1 \quad \textbf{(4.31)}$$

$$j\frac{\omega\mu}{k_C}AJ_0'(k_C\rho_1) = \frac{\omega\mu}{\sqrt{k_1\rho_1}}\frac{1}{k_1}(a_1-b_1) = \frac{\omega\mu}{\sqrt{k_1\rho_1}}\frac{(-1)}{k_1}\left(1+\frac{B}{A-K_j}\right)b_1 \quad \textbf{(4.32)}$$

$$j\frac{J_0'(k_C\rho_1)}{J_0(k_C\rho_1)}+\frac{k_C}{k_1}\frac{A+B-K_j}{A-B-K_j}=0 \qquad \textbf{(4.33)}$$

$$\frac{J_0'(k_C\rho_1)}{J_0(k_C\rho_1)}-j\frac{k_C}{k_1}\frac{K_j-A-B}{K_j-A+B}=0 \qquad \textbf{(4.34)}$$

4.1 Numerical Results

For the purpose of verification of the formulations and of their coding first a special problem is considered for which numerical solutions are given in the literature [9]. The particular problem to be considered is the determination of the transverse field distribution of the fundamental mode of a typical Bragg fiber with following parameters: n_c = 1.0, n_1 = 3, n_2 = 1.5, ρ_1 = 1 μm, l_1 = 0.130 μm, l_2 = 0.265 μm. For the above parameters equation (4.34) is used to find the dispersion of the fundamental TE mode in an air-core Bragg fiber.

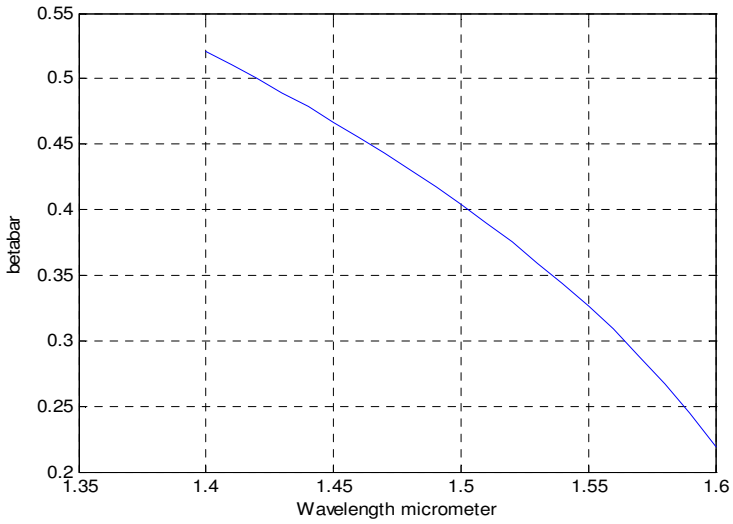

Figure 4.3 : Dispersion of the fundamental TE mode in an air-core Bragg fiber.

For wavelength which is equal to 1.55 μm has a betabar which is equal to 0.32635. Using these values H_Z and E_θ field of the guided TE mode at λ= 1.55 μm in the same Bragg fiber are found as:

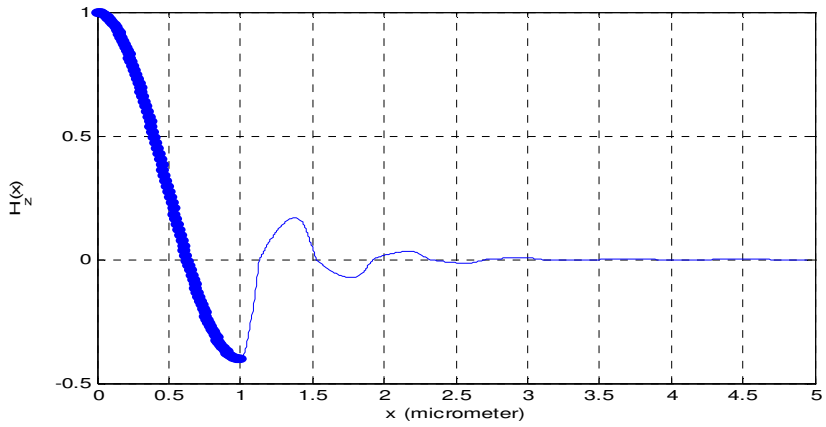

Figure 4.4 : H_Z field of the guided TE mode at λ= 1.55 μm in Bragg fiber, bold region shows the core thickness.

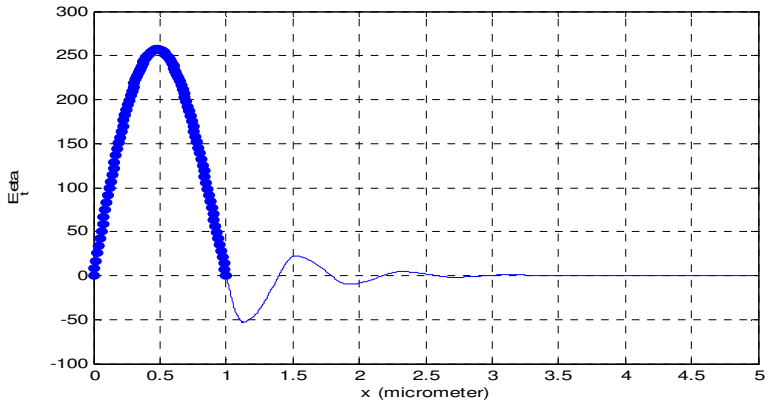

Figure 4.5 : E_θ field of the guided TE mode at λ= 1.55 μm in Bragg fiber, bold region shows the core thickness.

As shown in figures for this mode the field is relatively well guided within the "air-core" region and decays (albeit slowly) in an exponential manner away from it.

As a further example same parametres above are used to determine the variation of the dominant TM mode in Bragg fiber. The variation of E_Z field component and H_θ field component are shown in figure(4.6) and figure(4.7) respectively.

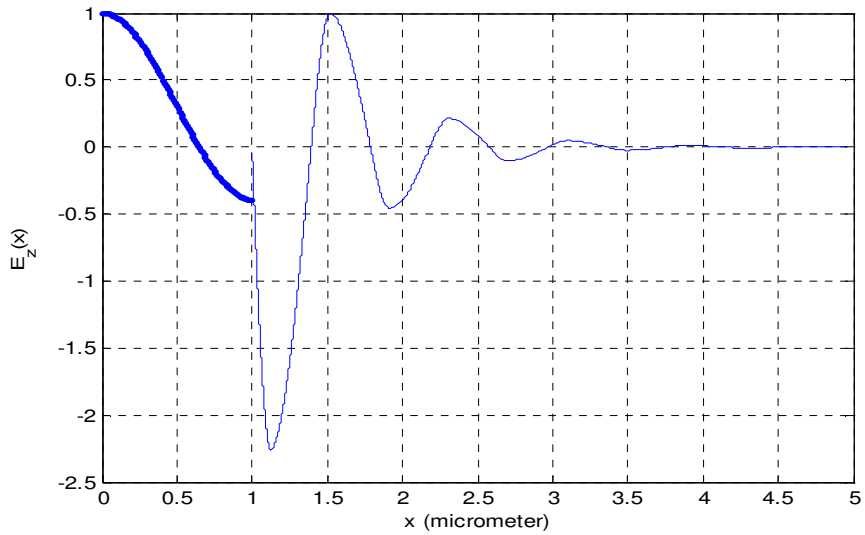

Figure 4.6 : E_Z field of the guided TM mode at λ= 1.55 μm in Bragg fiber, bold region shows the core thickness.

From figure (4.6) interfaces between the air-core in which field behaviour is shown in an exact form and the first cladding layer in which field is treated asymptotically, it is shown that the field of the last value of air-core region and the first value of the field in the first cladding layer do not coincide which indicates the presence of an ,yet unresolved, implementation problem.

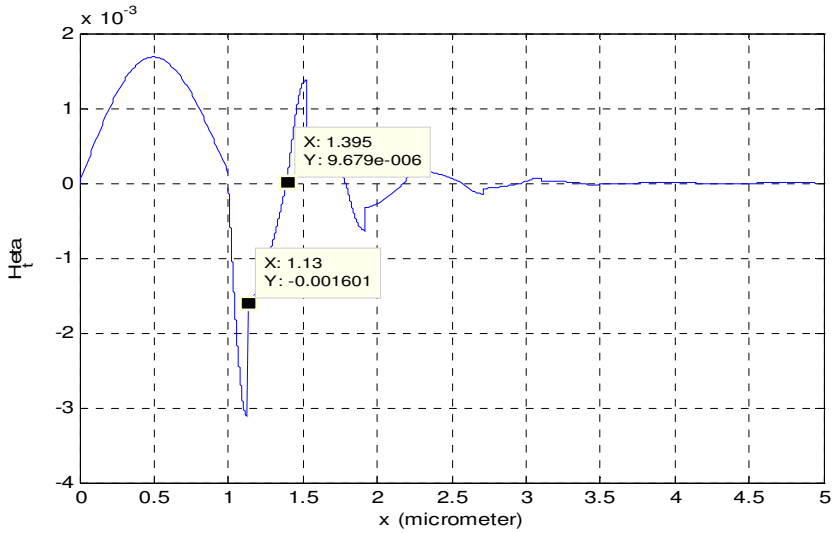

Figure 4.7 : H_θ field of the guided TM mode at λ= 1.55 μm in Bragg fiber, bold region shows the core thickness.

It should be noted that as expected, the slope of H_θ exhibits discontinuous at interfaces of cladding layers.

5. ASYMPTOTIC MATRIX THEORY OF BRAGG FIBER

In this approach the Bessel functions describing the fields in the first few layers of the cladding are kept intact and asymptotic expressions are used in the remaining layers [6].

Asymptotic approach can be refined by treating not only one but fist few layers can be solved in an exact way and the remainder can be solved by asymptotic approach. Formulas are explained before at chapter 2.3. By choosing the extent of the layers treated exactly the accuracy of calculations can be improved at the expense of added computational task.

For the purpose of verification of the formulations and of their coding first a special problem is considered for which numerical solutions are given in the literature [6]. The particular problem to be considered is the determination of the transverse field distribution of the fundamental hybrid mode of a typical Bragg fiber with following parameters: $n_c = 1.0$, $\rho_c = 1.0\Lambda$, $n_1 = 4.6$, $n_2 = 1.5$, $l_1 = 0.25\Lambda$, $l_2 = 0.75\Lambda$, $\omega = 0.286$ $(2\pi c/\Lambda)$. The azimuthal mode number is $l = 1$. The core region in asymptotic calculations consists of five dielectric layers, the air core and the first two cladding pairs. For the above parameters beta is found from equation (2.74) as $\beta = 0.129$ $(2\pi/\Lambda)$.

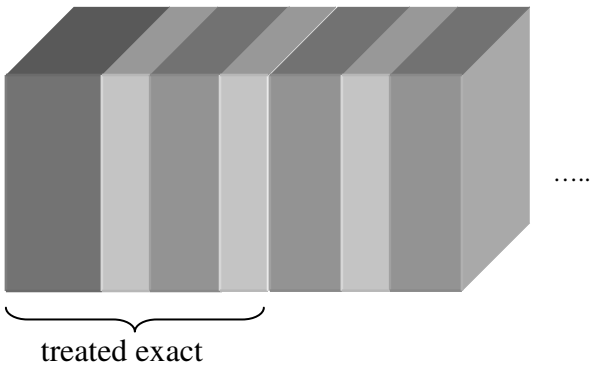

Figure 5.1 : Schematic of given numerical example.

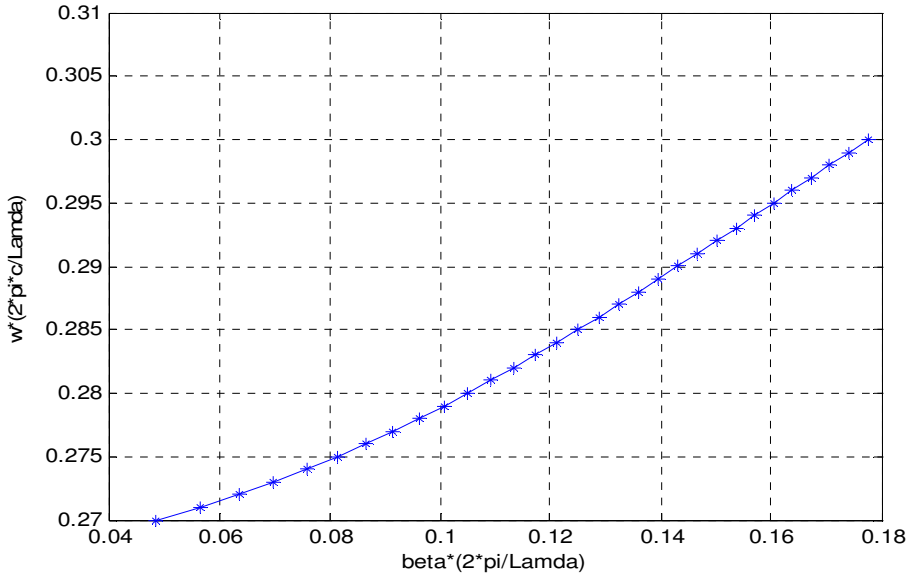

Figure 5.2 : The dispersion of the fundamental hybrid mode in an air core Bragg fiber.

Figure (5.2) is plotted by using the eigenvalue equation in (2.74). The field distribution of the guided Bragg fiber mode at $\omega = 0.286\ (2\pi c/\Lambda)$, the propagation constant is $\beta = 0.129\ (2\pi/\Lambda)$. Substituting the result into equation (2.75) and equation (2.76) the modal amplitude coefficients in the first layer of cladding region and in the center air core are found. The cladding fields are found from equation (2.47) to equation (2.54) and core fields are found by applying equation (2.30) and equation (2.31) repeteadly. The electromagnetic field distribution of the guided Bragg fiber mode with E_z and E_θ components and H_z and H_θ components are found as plotted figure (5.3) to figure (5.6).

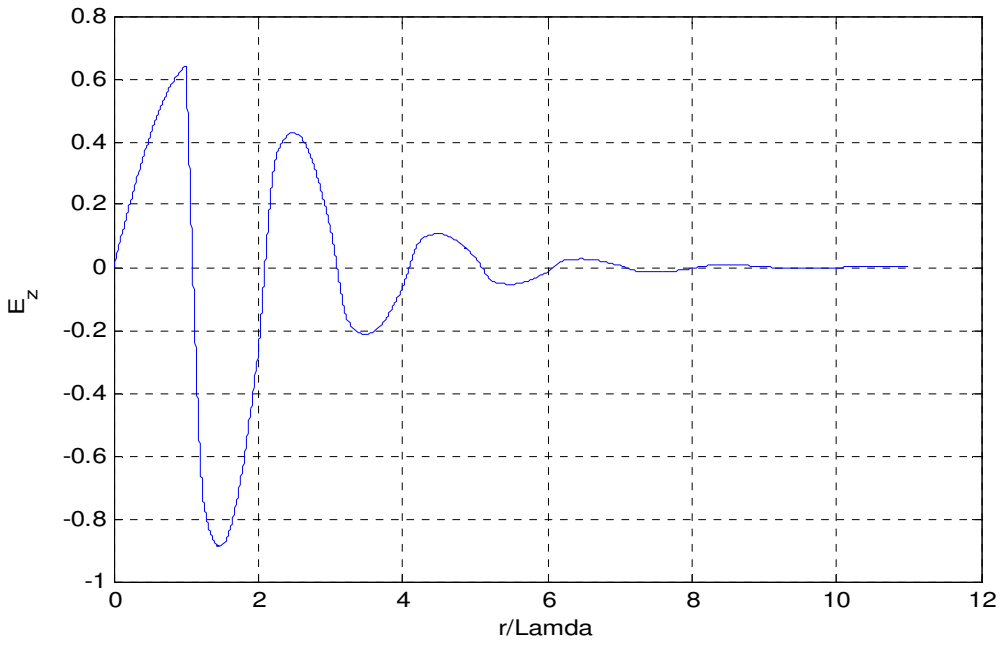

Figure 5.3 : The electromagnetic field distribution of the guided Bragg fiber mode with E_z component.

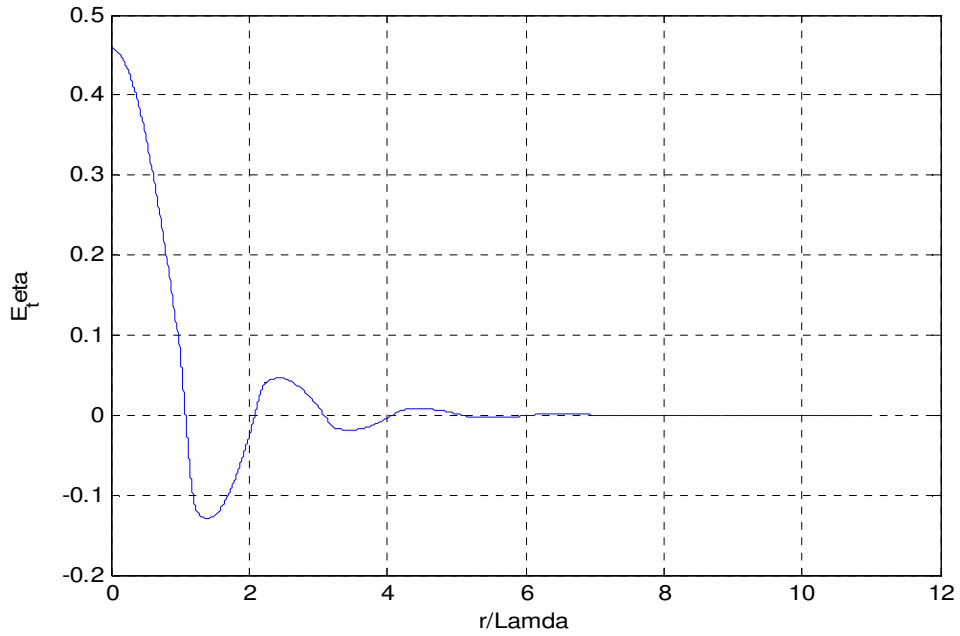

Figure 5.4 : The electromagnetic field distribution of the guided Bragg fiber mode with E_θ component.

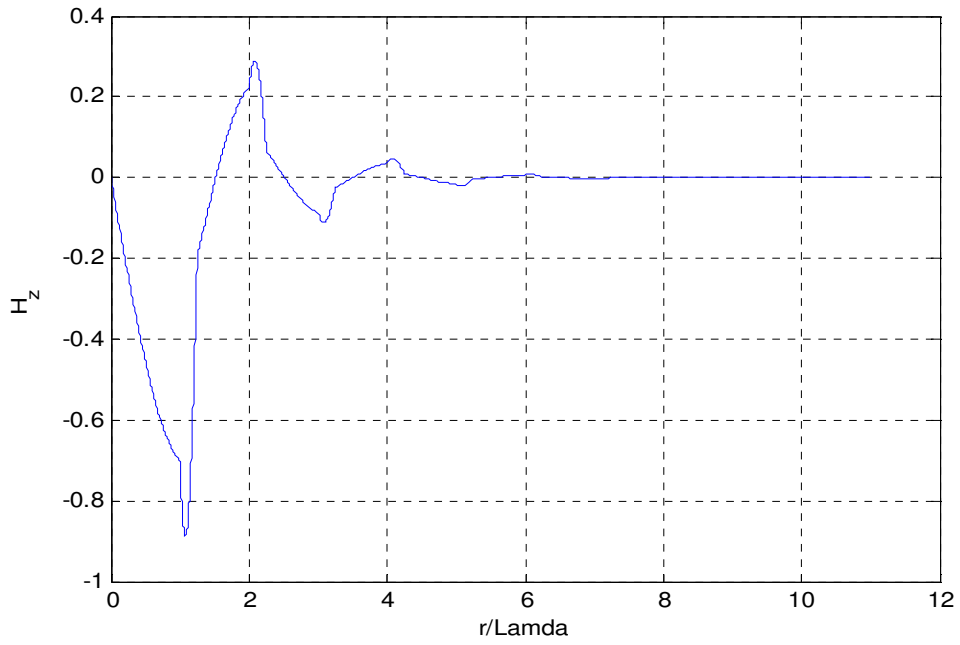

Figure 5.5 : The electromagnetic field distribution of the guided Bragg fiber mode with H_z component.

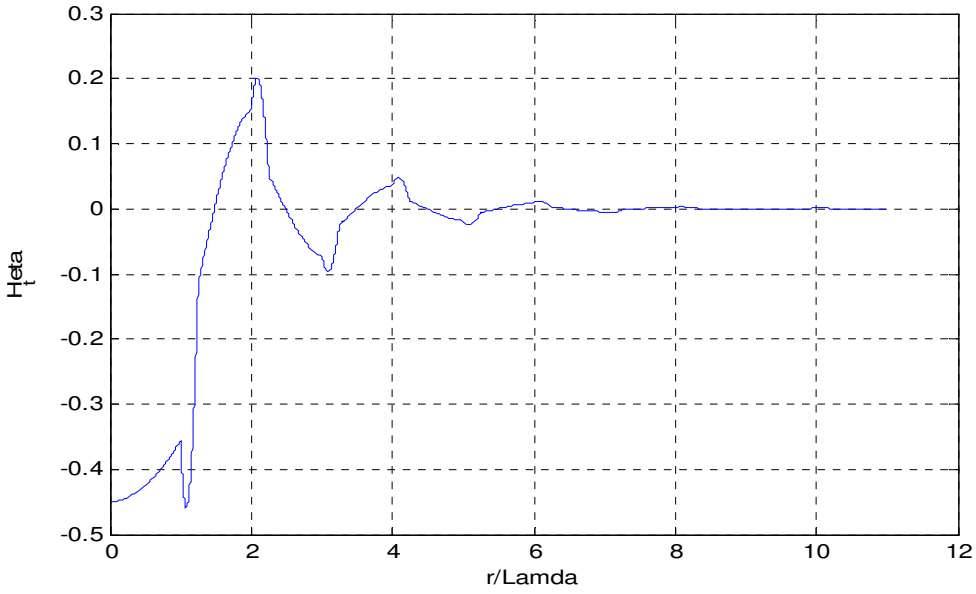

Figure 5.6 : The electromagnetic field distribution of the guided Bragg fiber mode with H_θ component.

6. CONCLUSION REMARKS AND FUTURE WORK

Due to the fact that most of the energy is confined to the 'air-core' the Bragg fibers provide following advantages:

- Practically eliminates dispersion, loss.
- Immune to nonlinear effects even at high power levels

However, due to increased cross-sectional dimensions and higher manufacturing costs they are not suited for long distance communication.

Today Bragg fibers are provided by some manufactures [12] and are used for certain specialized applications mostly in the medical domain.

Bragg fiber can be used to transmit a CO_2 laser (10.6μm) beam of sufficient intensity to the surgical area. This would have been rather difficult, if not impossible with other types of optical waveguides.

The analsis of Bragg fibers is complicated than that of conventional Bragg fibers. The analysis of Bragg fiber in an exact way the confined modes are treated as quasi-modes and their propagation constant and field distribution are found by minimizing the radiation loss [5]. For transverse electric and transverse magnetic modes, solution of exact analysis is relatively easy, because the radiation loss depends only on propagation constant but for other types this approach becomes complicated since finding the eigenmode in fiber cladding layers is difficult. Eigensolutions of a planar Bragg waveguide can be found easily. Bloch theorem can be applied to a planar Bragg waveguide since it exhibits a perfect, discrete translational symmetry. Bloch theorem does not apply for a Bragg fiber which has cylindrical symmetry.

At the turn of this millennium it was recognized that by using asymptotic expressions, rather than exact ones for the Bessel functions with large arguments the formulation can be cast into an eigenvalue problem that can be solved in a numerically efficient way.

In the historical sequence the first investigation treated the entire cladding region asymptotically which was then refined by not using asymptotic in the first few cladding layers. The difference between the asymptotic results and results obtained from minimizing radiation loss is less than 2% for a Bragg fiber with small air core radius comparable to the wavelength.

Bragg fibers have received considerable attention in the last decade [5-9] due to some potential advantages they may provide in certain applications. The problem can not be formulated exactly in the strict sense. Several approximate techniques have been introduced for their analysis. In this work, the transfer matrix method is investigated which is the most accurate approach since the error in the calculations can be reduced arbitrarily by increasing the number of layers retained in exact formulation. The presented analyses follows closely those reported by A. Yariv and his co-workers [5-6,8-9] and contains the details of formulation, replication of the numerical results as well as some minor extensions (TM modes in planar stack, odd – even modes etc.).

The calculation of propagation characteristics of Bragg fibers presents a challenging numerical task. This is due to the fact that the presence/absence of air guided modes is critically dependent on the parameters of the waveguide. Moreover, there are generally multiplicities of supported modes which are almost always confined to narrow β intervals. We have found that a very slight change in any parameter of the waveguide may result in complete disruption of the modal field behavior.

Another contribution of this work is the introduction of multi-layer cladding structures, for which the formulation is derived for a 3-layer structure, in a form extendable to arbitrary number of layers. It is believed that the introduction of additional layers will allow better control of transmission characteristic.

Following areas are identified as follow-up open problems.

1. A systematic approach for synthesizing Bragg fibers (determining the waveguide parameters) with given propagation characteristics.
2. Continue work on multi-layer structures.

REFERENCES

[1] **Joannopoulos, J. D., Meade, R. D. and Winn, J., N.,** 1995. Photonic Crystals. Princeton University Press, Princeton.

[2] **Yablonovitch, E.**, 1987. Inhibited spontaneous emission in solid-state physics and electronics, *Physical Review Letters,* **58**, 2059-2062.

[3] **John, S.**, 1987. Strong localization of photons in certain disordered dielectric superlattices, *Physical Review Letters,* **58**, 2486-2489.

[4] **Bjarklev, A., Broeng J. and Bjarklev, A.S**., 2003. Photonic Crystal Fibres. Kluwer Academic Publishers, USA.

[5] **Yeh, P.**, **Yariv, A., and Marom, E.,** 1978. Theory of Bragg Fiber, *Optical Society of America,* **68**, 1196-1201.

[6] **Xu, Y.**, **George, X., Lee, K. R., Member, IEEE, and Yariv, A., Life Fellow, IEEE,** 2002. Asymptotic Matrix Theory of Bragg fibers, *Journal of Lightwave Technology,* **20**, 428-440.

[7] **Ibanescu, M.**, **Fink, Y., Fan, S., Thomas, E. L. and Joannopoulos, J. D.,** 2000. An all-dielectric coaxial waveguide, *Science,* 289, 415-419.

[8] **Yeh, P.**, **Yariv, A.,** 1976. *Optics Communication,* **19**, 427.

[9] **Xu, Y.**, **Lee, K. R. and Yariv, A.,** 2000. Asymptotic analysis of Bragg fibers, *Optics Letters,* **25**, 1756-1758.

[10] **Sakai, J.**, **Nouchi, P.,** 2005. Propagation properties of Bragg fiber analyzed by a Hankel function formalism, *Optics Communication,* **249**, 153-163.

[11] **Sakoda, K.**, 2005. Optical Properties of Photonic Crystals. Springer, Germany.

[12] http://www.omni-guide.com

[13] **Zhi, W., Guobin, R., Shugin , L., Weijun, L., Guo, S.,** 2003. Compact supercell method based on opposite parity for Bragg fibers, *Optics Express*, **11**, 3542-3549.

[14] **Sakai, J., Sasaki, J.,** 2006. Hybrid modes in a Bragg fiber: dispersion relation and electromagnetic fields, *Journal of Optical Society of America*, **23**, 1020-1028.

APPENDIX : BLOCH THEOREM

Photonic crystals have discrete translational symmetry which means they are invariant under translation of any distance; instead they are invariant under translation of any distance which is a multiple of some fixed step length.

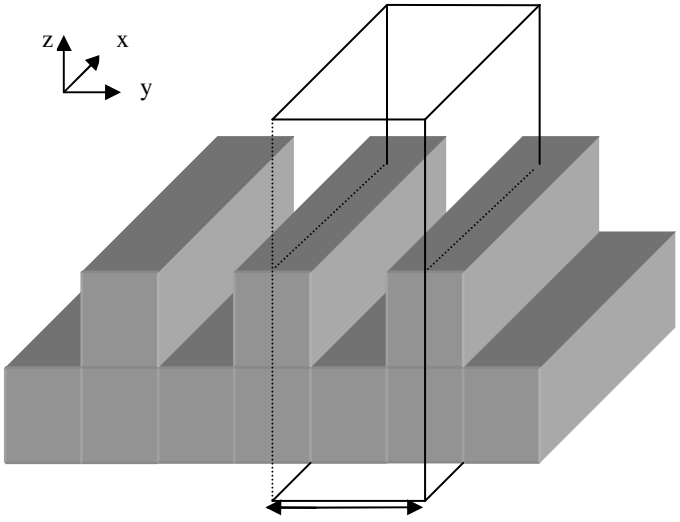

Figure A.1 : A dielectric configuration with discrete translation symmetry.

A structure shown in figure (A.1) we have continuous translational symmetry in the x-direction and discrete translational symmetry in the y-direction. The symbol 'a' that is shown in the figure above, is lattice constant. Because of the symmetry of the structure ε(r) = ε(r+a) and also ε(r) = ε(r+R) in which R=la, where l is an integer. These systems eigenfunctions are plane waves [1]:

$$T_R \exp(ik_y y) = \exp(ik_y (y + la)) = \exp(ik_y la)\exp(ik_y y) \quad \textbf{(A.1)}$$

$$T_{dx} \exp(ik_x x) = \exp(ik_x (x + d)) = \exp(ik_x d)\exp(ik_x x) \quad \textbf{(A.2)}$$

If we look at the different k_y values, example if the first one is k_y and the other equals (k_y+2Π/a), one can show that these are not different from each other. Also,

(k_y+m2Π/a) in which k is an integer shows the same T_R eigenvalue of exp(i($k_y$la)). Because of this property, we can show the original modes as:

$$H_{kx,ky}(r) = \exp(ik_x x)\sum_m c_{ky} m(z)\exp\left(i\left(k_y + mb\right)y\right)$$

$$= \exp(ik_x x)\exp(ik_y y)\sum_m c_{ky} m(z)\exp(imby)$$

$$= \exp(ik_x x)\exp(ik_y y)u_{ky}(y,z) \qquad \textbf{(A.3)}$$

Where b = 2Π/a, c are coefficient numbers which comes from explicit solution, u(y, z) is a periodic function in y-direction. When we use u(y+la, z), we see that it is equal to u(y, z). Under these explanations we can see that H is a product of plane wave with a 'y' periodic function. This property is known as Bloch's theorem. In solid-state physics it is called Bloch state, and in mechanics it is known as Floquet mode.

Bloch or equally Floquet theorem says that waves can propagate without scattering, whether waves consist of electrons or of light beams, in a periodic medium [11].

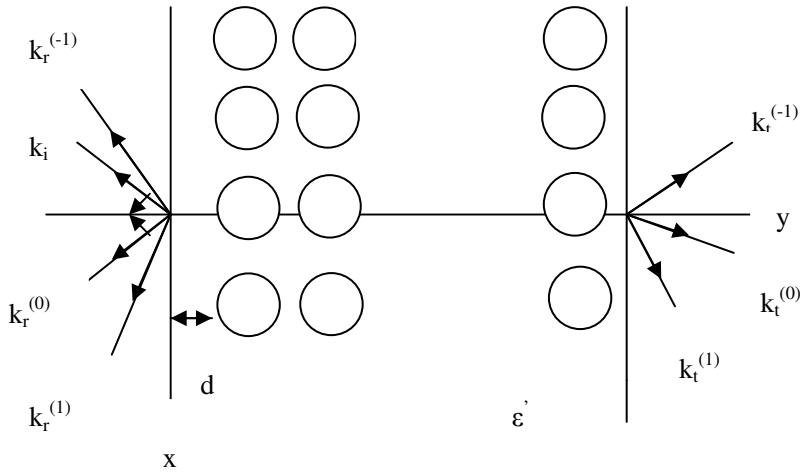

Figure A.2 : Configuration for the calculation of the transmission and the Bragg reflection spectra (top view).

BIOGRAPHY

Aslı Ünlügedik was born in Kahramanmaraş, Turkey in 1979. She received the B.Sc. degree in electrical and electronics engineering from Yeditepe University. In 2004, she enrolled the M.Sc. degree at Istanbul Technical University.